Statistics for Gaussian Random Fields with Unknown Location and Scale using Lipschitz-Killing Curvatures

Elena Di Bernardino, Céline Duval

Statistics for Gaussian Random Fields with Unknown Location and Scale using Lipschitz-Killing Curvatures

Elena Di Bernardino*, Céline Duval†

Abstract

In this paper we study some statistics linked to the average of Lipschitz-Killing (LK) curvatures of the excursion set of a stationary non-standard isotropic Gaussian field X on $\mathbb{R}^2$. Under this hypothesis of unknown location and scale parameters of X, we introduce novel fundamental quantities, that we call *effective level* and *effective spectral moment*, and we derive unbiased and asymptotically normal estimators of these parameters. Furthermore, empirical variance estimators of the asymptotic variance of the third LK curvature of the excursion set (*i.e.*, the area) and of the *effective level* are proposed. Their consistency is established under a weak condition on the correlation function of X. Finally, using the previous asymptotic results, we built a test to determine if two images of excursion sets can be compared. This test is applied on both synthesized and real mammograms.

Key words: Gaussian random fields, Excursion sets, Euler characteristic, Test of Gaussianity, Image analysis.

AMS Classification: 60G60, 62F12, 62F03, 62M40.

1 Introduction

Lipschitz-Killing (LK) curvatures are geometrical objects which permit to analyse d dimensional objects. Considering a black and white image in dimension $d = 2$, there are three LK curvatures: the surface area, the half perimeter and the Euler characteristic. Each of them brings a distinct information on the geometry of the black (resp. white) zone. The surface area is related to its occupation density, the perimeter to its regularity and the Euler characteristic to its connectivity.
In this paper, the images we consider are the excursion sets of the realization of a two-dimensional Gaussian stationary and isotropic random field X above a given level u, *i.e.* a black and white image indicating when the realization of X is above or below the level u. Using random fields in the modelization and analyzing their realizations with LK curvatures has been successfully exploited in many disciplines. In cosmology, to study the Cosmic Microwave Background radiation (see, *e.g.*, Casaponsa et al. (2016), Schmalzing and Górski (1998), Gott et al. (2007)) or to analyze the distribution of galaxies (see, *e.g.*, Gott et al. (2008)). The LK curvatures are also exploited in brain imaging (see Adler and Taylor (2011), Section 5, and the references therein) or to model sea waves (see, *e.g.*, Longuet-Higgins (1957), Wschebor (2006), Lindgren (2000)).

The average LK curvatures of the excursion set have been studied in a wide variety of contexts and depending on the nature of the underlying fields X, they can be computed explicitly (see Adler and Taylor (2007, 2011), Biermé et al. (2019); see also Adler et al. (2012) for a focus on the Gaussian kinematic

*Conservatoire National des Arts et Métiers, Paris, EA4629, 292 rue Saint-Martin, Paris Cedex 03, France; elena.dibernardino@lecnam.net

†MAP5 UMR 8145, Université Paris Descartes, 45 rue des Saints-Pères, Paris, France; celine.duval@parisdescartes.fr

formula et Biermé and Desolneux (2016) in case X is a shot noise). The (empirical) LK curvatures computed on an excursion set have also been studied when the size of the observation window increases. Specific asymptotic results have been established in several cases and these results highly depend on the nature of the underlying field X and the LK curvature considered (in the standard Gaussian random field framework, see *e.g.*, Estrade and León (2016) or Di Bernardino et al. (2017) for the Euler characteristic; Bulinski et al. (2012) or Pham (2013) for the area also called sojourn times, Kratz and Vadlamani (2018), Müller (2017) for the asymptotic joint study of all LK curvatures at the same time; in the random fields defined on a discrete space framework, see *e.g.*, Hug et al. (2016), Lachièze-Rey (2017), Ebner et al. (2018)).
These asymptotic results can be considered as a starting point to derive consistent parameter estimators and tests for the underlying field X (see Di Bernardino et al. (2017), Biermé et al. (2019), Berzin (2018)). Note that inference methods and tests using LK curvature devices only rely on the sparse observation of one excursion set and not on the covariance function nor on the marginal distribution of the field that require the observation of the entire field. For this latter type of testing procedures the reader is referred for instance to Epps (1987), Pantle et al. (2010), Nieto-Reyes et al. (2014).

Asymptotic variance estimation One practical problem encountered when calibrating testing procedures or studying the deviations of the estimators is that these quantities often depend on the unknown asymptotic variances of the empirical LK curvatures. Having estimators of this asymptotic variance is crucial for the statistical study of these objects, to control the deviation of the estimated quantities with respect to their actual value and to build consistent statistical procedures. Estimation strategies are known and used in practice in a wide range of contexts, even though there are few theoretical results. Their consistency is established only in the case of the area if X is a Gaussian random field and under conditions on the correlation function of X that are difficult to check (see Mattfeldt et al. (2011), Bulinski et al. (2012)).

In case X is a stationary and isotropic Gaussian field whose correlation function decays polynomially (see Assumption ($\mathcal{A}1$) below), using the Itô-Wiener decomposition of Itô-Wiener chaos of the LK curvatures jointly with the diagram formula (see Taqqu (1977)), we propose a consistent empirical variance estimator for the empirical area. We also argue why this estimator should remain consistent to estimate the Euler characteristic variance.

Removing the known mean and variance assumption If X is a stationary and isotropic Gaussian random field, excursion sets can be easily simulated and the global properties of the simulated images can be directly related to the model parameters. A large literature has been developed concerning known mean and variance stationary Gaussian random field (typically zero mean and unit variance).
However, it seems more realistic and less restrictive in the real-life applications to consider images with unknown location and scale parameters. Indeed, assuming that the field is, *e.g.*, centered with unit variance, imposes (in particular if the field is symmetric, which is the case of Gaussian fields) that the Euler characteristic of the set is null at level $u = 0$ and that its area is $1/2$ at this same level. Worse, if one has only the observation of an excursion set –and not the whole field– it is often impossible to test whether the underlying field is centered or has unit variance. It is neither possible to estimate its mean and variance from the only observation of the excursion set.

We focus on the more realistic setting of a stationary and isotropic Gaussian random field with unknown location and scale parameters (see Assumption ($\mathcal{A}0$) below). This context has deserved only a few attention in the literature, we can mention, for instance, David and Worsley (1995) based on the Hadwiger characteristic. This modification that may appear minor, in fact removes all the information on the

scaling of the field and on the locations where the excursion set shows black and white zones in comparable proportions. In order to compare geometries of two given excursion sets, this information turns out to be crucial and can be estimated from the LK curvatures via two quantities that we introduce in the present paper and that we call in the sequel *effective level* and *effective spectral moment* of the field (see Proposition 1.1, below). They contain simultaneously the knowledge of the variance and mean of the field and of the observation level u of the considered excursion set. Notice that, if the underlying Gaussian field X is centered with unit variance, the *effective level* simply coincides with the observation level u and the *effective spectral moment* with the spectral moment of X.

Comparing images of exclusion sets We underline that, when one wishes to compare two different fields from the observation of one excursion set of each, observing them at the same level u is irrelevant if the underlying fields have distant mean and/or variance. On the contrary if these excursion sets are observed the same *effective level* and *effective spectral moment*, comparing them using LK curvature devices is meaningful. This behavior can be visualized in Figure 3 (left) below. This is why in Section 4.1 we propose a consistent test to decide whether two images of excursion sets have the same *effective level* or not. The construction of this test makes a full use of the asymptotically normal estimator of *effective level* as well as the consistent estimator of its limit variance, introduced in the present work.

Main contributions of the paper In this article, we are mainly interested in the Euler characteristic and area as they are numerically more stable to compute (see, *e.g.*, the discussion about the well known numerical instability of the perimeter estimation in Biermé et al. (2019)). Moreover, as we prove results on the asymptotic variance of the area, the numerical results in Section 4.1 rely only on this latter quantity.

To sum up, the contributions of this paper are the following.

1. We introduce the notions of *effective level* and *effective spectral moment* for stationary non-standard isotropic Gaussian fields. From the formulae of the average LK curvatures of the excursion sets of such fields, we derive unbiased and asymptotically normal estimators of the *effective level* and the *effective spectral moment* (see Propositions 2.1 and 2.2).

2. We propose an empirical variance estimator of the asymptotic variance of the area and of the *effective level* and we establish their consistency (see main Theorem 3.1 and Corollary 3.1) under a weak condition on the correlation function of the field X (see Assumption $(\mathcal{A}1)$). Furthermore, we provide arguments (see Conjectures 3.1 and 3.2) why the empirical variance estimator of the Euler characteristic should also be consistent under an additional decay assumption (see Assumption $(\mathcal{A}3)$).

3. We provide a test to determine if two images of excursion sets are comparable using LK curvatures or not (see Corollary 4.1). The performances and the practical usefulness of this test is discussed on both synthesized and real mammograms.

Outline of the paper The paper is organized as follows. In the remaining of this section we define the three objects of interest, *i.e.*, the LK densities for the excursion sets of a two-dimensional Gaussian random field which is non centered and whose variance is not necessarily one. These formulae depend on two identifiable parameters, called *effective level* and *effective spectral moment*. In Section 2 we estimate these parameters and establish asymptotic normality results. The associated asymptotic variances are estimated in Section 3, using a subwindow technique. The consistency of the proposed subwindow

empirical variance estimators is studied in Section 3.1 as well as some statistical implications in Section 3.2. In Section 4 we build a test based on the *effective level* to compare two images of excursion sets. This test is put into practice in Section 4.1 on synthesized 2D digital mammograms provided by GE Healthcare France (department Mammography) and in Section 4.2 on real digital mammograms provided by the Mammographic Image Analysis Society (MIAS). Finally, two appendix sections gather the proofs of the technical results (Appendix A) and some additional numerical results (Appendix B).

1.1 Definitions and preliminary notions

In the whole paper, $|.|$ denotes equally the absolute value or the two dimensional Lebesque measure and by $|\cdot|_1$ its one-dimensional Hausdorff measure, $\|.\|$ denotes the Euclidian norm. We consider X being a Gaussian field defined on $\mathbb{R}^2$ satisfying the following hypothesis.

($\mathcal{A}0$) The Gaussian field X is stationary, isotropic with mean $\mathbb{E}[X(0)] = \mu$, variance $\mathbb{V}(X(0)) = \sigma^2$ and $\mathbb{V}(X'(0)) = \lambda I_2$ for $\lambda > 0$, the second spectral moment, $\sigma > 0$, $\mu \in \mathbb{R}$ and I_2 the 2×2 identity matrix. Moreover, the trajectories of X are almost surely of class C^3.

Denote by r the covariance function of X, *i.e.*, for any fixed t, $r(t) = \mathrm{Cov}(X(0), X(t))$ and by ρ the correlation function $\rho(t) = \mathrm{corr}(X(0), X(t))$. Under Assumption ($\mathcal{A}0$) the field is suppose to be C^3, then the covariance function is C^6. In some cases, *e.g.*, to get the asymptotic normality or consistency of our estimators, we impose additional assumptions on covariance and correlation functions of X gathered in the following.

($\mathcal{A}1$) $t \mapsto \rho(t)$ is decreasing and $|\rho(t)| \leq (1 + \|t\|)^{-\gamma}$, $\gamma > 2$.

($\mathcal{A}2$) For any fixed t in $\mathbb{R}^2$, the covariance matrix of the random vector $(X(t), X^{'}(t), X^{''}(t))$ has full rank and the covariance function r of X is such that,

$$\int_{\mathbb{R}^2} r(s)\,\mathrm{d}s > 0, \quad M_r(t) \to 0 \ \text{ when } \ \|t\| \to +\infty \quad \text{and} \quad M_r \in L^1(\mathbb{R}^2)\,,$$

where

$$M_r(t) = \max\left(\left|\frac{\partial^{\mathbf{k}}}{\partial t^{\mathbf{k}}} r(t)\right|;\, \mathbf{k} = (i_1, \ldots, i_\ell) \in \{1,2\}^\ell,\, 0 \leq \ell \leq 4\right)$$

and $\frac{\partial^{\mathbf{k}} r}{\partial t^{\mathbf{k}}}(t) = \frac{\partial^\ell}{\partial x_{i_1} \ldots \partial x_{i_\ell}} r(t)$.

Assumptions ($\mathcal{A}0$), ($\mathcal{A}1$) and ($\mathcal{A}2$) are standard when studying limit laws of non linear functionals of stationary Gaussian random fields.

Rectangles, denoted by T, in $\mathbb{R}^2$ are bounded and with non empty interior. In the following notation $T \nearrow \mathbb{R}^2$ stands for the limit along any sequence of bounded rectangles that grows to $\mathbb{R}^2$. For that, set $N > 0$ and define

$$T^{(N)} := \{Nt : t \in T\}$$

the image of a fixed rectangle T by the dilatation $t \mapsto Nt$ and then letting $T \nearrow \mathbb{R}^2$ is equivalent to $N \to \infty$. Then, $T^{(N)}$ is a Van Hove-growing sequence (VH-growing sequence, see Definition 6 in Bulinski et al. (2012)), *i.e.*, $|\partial T^{(N)}|_1 / |T^{(N)}| \to 0$ as $N \to \infty$, where ∂T stands for the frontier of the set T. In the sequel, we sometimes drop the dependency in N of the rectangle T to soften notation.

1.2 Lipschitz-Killing curvatures of a given excursion set

Let $u \in \mathbb{R}$. For X a real-valued stationary random field defined on $\mathbb{R}^2$, we consider the excursion set within T above level u:

$$\{t \in T \,:\, X(t) \geq u\} = T \cap E_X(u), \quad \text{where } E_X(u) := X^{-1}([u, +\infty)).$$

Definition 1.1 (LK curvatures of $E_X(u)$)**.** *Let X be a Gaussian field satisfying Assumption (A0). Define the following Lipschitz-Killing curvatures for the excursion set $E_X(u)$, for $u \in \mathbb{R}$,*

$$\mathcal{L}_2(X, u, T) := |T \cap E_X(u)| = \int_T \mathbf{1}_{\{E_X(u)\}}(t)\, \mathrm{d}t, \tag{1}$$

$$\mathcal{L}_1(X, u, T) := |\partial(T \cap E_X(u))|_1 = \frac{1}{2} \lim_{\varepsilon \to 0} \int_T \delta_{]u-\varepsilon, u+\varepsilon[}(X(t))\, \|\nabla X(t)\|\, \mathrm{d}t, \tag{2}$$

$$\mathcal{L}_0(X, u, T) := \sharp \text{ connected components in } T \cap E_X(u) - \sharp \text{ holes in } T \cap E_X(u), \tag{3}$$

$$= \frac{1}{|T|} \left(\sharp(T \cap \mathcal{C}_{extr.}) - \sharp(T \cap \mathcal{C}_{saddle}) \right), \tag{4}$$

where $\mathcal{C}_{extr.} = \big\{t : X(t) \geq u, \nabla X(t) = 0,\ t \text{ is a local extremum}\big\}$, $\mathcal{C}_{saddle} = \big\{t : X(t) \geq u, \nabla X(t) = 0,\ t$ is a saddle point$\big\}$, δ_u the Dirac mass at u and ∇X is the gradient field.

These three additive functionals, $\mathcal{L}_j$ for $j = 0, 1, 2$ in Definition 1.1 are called in the literature intrinsic volumes, Minkowski functionals or Lipschitz-Killing curvatures. Roughly speaking, for A a Borelian set in $\mathbb{R}^2$, $\mathcal{L}_0(A)$ stands for the Euler characteristic of A, $\mathcal{L}_1(A)$ for the half perimeter of the boundary of A and $\mathcal{L}_2(A)$ is equal to the area of A, *i.e.*, the two-dimensional Lebesgue measure.

In particular, when T is a bounded rectangle in $\mathbb{R}^2$ with non empty interior,

$$\mathcal{L}_0(T) = 1, \quad \mathcal{L}_1(T) = \frac{1}{2}|\partial T|_1, \quad \mathcal{L}_2(T) = |T|. \tag{5}$$

Using the same formalism as in Biermé et al. (2019), the normalized LK curvatures are given by

$$C_i^{/T}(X, u) := \frac{\mathcal{L}_i(X, u, T)}{|T|}, \quad \text{for } i = 0, 1, 2,$$

and the associated LK densities by

$$C_i^*(X, u) := \lim_{T \nearrow \mathbb{R}^2} \mathbb{E}[C_i^{/T}(X, u)], \quad \text{for } i = 0, 1, 2. \tag{6}$$

In the case $i = 2$, one can easily write $C_2^*(X, u) = \mathbb{E}[C_2^{/T}(X, u)] = \mathbb{P}(X(0) \geq u)$. Computationally $C_2^{/T}(X, u)$ $C_1^{/T}(X, u)$ and $C_0^{/T}(X, u)$ in (1), (2) and (3) can be evaluated in a given image by using the Matlab functions `bwarea`, `bwperim` and `bweuler` respectively. The numerical evaluation of (4) can be obtained for instance by finding local maxima, local minima and saddle points with the Matlab function `imextrema`.

Definition 1.2. *Let X be a Gaussian random field satisfying Assumption (A0). We define the effective observation level (effective level in the sequel)*

$$s_u := \frac{u - \mu}{\sigma}$$

and the effective second spectral moment (effective spectral moment in the sequel) of the field X

$$a := \frac{\lambda}{\sigma^2}.$$

Using s_u and a as in Definition 1.2, we now compute the expected value of these empirical LK curvatures of excursion sets of a Gaussian random field with unknown location and scale and derive the corresponding LK densities.

Proposition 1.1. *Let X be a Gaussian random field satisfying Assumption (A0), denote $\psi(x) = \mathbb{P}(\mathcal{N}(0,1) \geq x)$. Then, it holds that*

$$\mathbb{E}[C_0'^T(X,u)] = \frac{\psi(s_u)}{|T|} + \frac{\sqrt{a}}{2\pi}\exp\left\{-\frac{1}{2}s_u^2\right\}\frac{|\partial T|_1}{2|T|} + \frac{a}{(2\pi)^{3/2}}\exp\left\{-\frac{1}{2}s_u^2\right\}s_u,$$
$$\mathbb{E}[C_1'^T(X,u)] = \psi(s_u)\frac{|\partial T|_1}{2|T|} + \frac{\sqrt{a}}{4}\exp\left\{-\frac{1}{2}s_u^2\right\},$$
$$\mathbb{E}[C_2'^T(X,u)] = \psi(s_u).$$

Having $T \nearrow \mathbb{R}^2$, it follows that the LK densities defined in (6) are given by

$$C_0^*(X,u) = \frac{a}{(2\pi)^{3/2}}\exp\{-\frac{1}{2}s_u^2\}s_u, \quad C_1^*(X,u) = \frac{\sqrt{a}}{4}\exp\{-\frac{1}{2}s_u^2\}, \quad C_2^*(X,u) = \psi(s_u). \tag{7}$$

Proof of Proposition 1.1 is postponed to Section A.2.

Remark 1 (Unbiased estimators for LK densities)**.** Let $u \in \mathbb{R}$ and X be a stationary isotropic Gaussian random field defined on $\mathbb{R}^2$ satisfying Assumption (A0). Assume we observe $T \cap E_X(u)$ for T a rectangle in $\mathbb{R}^2$. The following quantities are unbiased estimator of $C_i^*(X,u)$ in (7) (see also Biermé et al. (2019)):

$$\widehat{C}_{2,T}(X,u) = C_2'^T(X,u), \tag{8}$$
$$\widehat{C}_{1,T}(X,u) = C_1'^T(X,u) - \frac{|\partial T|_1}{2|T|}C_2'^T(X,u), \tag{9}$$
$$\widehat{C}_{0,T}(X,u) = C_0'^T(X,u) - \frac{|\partial T|_1}{\pi|T|}C_1'^T(X,u) + \left(\frac{1}{2\pi}\left(\frac{|\partial T|_1}{|T|}\right)^2 - \frac{1}{|T|}\right)C_2'^T(X,u), \tag{10}$$

2 Estimators of the *effective level* s_u and *effective spectral moment* a

We focus on stationary Gaussian random fields with unknown location and scale parameters. From the LK densities given by (7) only s_u and a are identifiable. Comparing these values with the case of a centered field with unit variance, one can consider s_u as *effective observation level* (*effective level* in the sequel) and a as the *effective spectral moment* of the field X. Indeed, a comparison between two images (with unknown and eventually different location and scale parameters) can be proposed by using excursion sets and relative LK curvatures only if the considered level of the excursion set makes sense in terms of mean and variance. In this sense, for a given $u \in \mathbb{R}$, the level (*resp.* spectral moment) of interest is the unknown s_u (*resp.* a) appearing Proposition 1.1. Remark that the LK densities C_i^* in Proposition 1.1 only depend on these two parameters. In this section we build consistent estimators for s_u and a in Definition 1.2 relying on (8), (10) and Proposition 1.1.

Definition 2.1 (Estimators for s_u and a)**.** *Define the estimator of s_u built on the observation $T \cap E_X(u), u$ being fixed, by* $\arg\min_{s\in\mathbb{R}} |\psi(s) - \widehat{C}_{2,T}(X,u)|$*, i.e.*

$$\widehat{s}_{u,T} := \psi^{-1}(\widehat{C}_{2,T}(X,u)). \tag{11}$$

Let T_1 and T_2 be two rectangles in T such that $dist(T_1, T_2) > 0$ and $|T_1| = |T_2| > 0$. Define the estimator of a built on the observation $T \cap E_X(u), u \neq \mu$ being fixed, by

$$\widehat{a}_{u,T} := \frac{\widehat{C}_{0,T_1}(X,u)(2\pi)^{3/2}}{\widehat{s}_{u,T_2}\,\exp\{-\frac{1}{2}(\widehat{s}_{u,T_2})^2\}}. \tag{12}$$

Remark 2 (Bias for $\widehat{s}_{u,T}$ and $\widehat{a}_{u,T}$)**.** Estimator $\widehat{s}_{u,T}$ in (11) is the quantile of the standard Gaussian distribution at random level $1 - \widehat{C}_{2,T}(X,u)$, where $\widehat{C}_{2,T}(X,u)$ defined in (8) is unbiased. It follows that $\widehat{s}_{u,T}$ is biased, as the function ψ^{-1} is convex in $(0, 0.5)$ (*resp.* concave in $(0.5, 1)$), then it holds $\mathbb{E}[\widehat{s}_{u,T}] > s_u$ if $\widehat{C}_2^{/T}(X,u)$ in (0,0.5) (resp. $\mathbb{E}[\widehat{s}_{u,T}] < s_u$ if $\widehat{C}_2^{/T}(X,u)$ in (0.5,1)). The bias of $\widehat{s}_{u,T}$ certainly generates a bias also in the estimation of a. This bias for $\widehat{s}_{u,T}$ can be assessed in Figure 9 (see Appendix B).

Remark 3. Let X be a stationary random field, non necessarily Gaussian, with finite variance. It holds $\mathbb{E}[C_2^{/T}(X,u)] = \mathbb{P}(X(0) \geq u) = \mathbb{P}\big(\frac{X(0)-\mu}{\sigma} \geq s_u\big) =: F(s_u)$. Then, given a family for the marginal distribution F of the field, known up two its first two moments, the *effective level* of the field can always be recovered using $\widehat{s}_u = F^{-1}(C_2^{/T}(X,u))$. This is not derived from the kinematic formula contrary to the equation leading to the computing of a.

Proposition 2.1 (Asymptotic normality of $(\widehat{s}_{u_1,T}, \ldots, \widehat{s}_{u_m,T})$)**.** *Let X be a Gaussian random field satisfying Assumptions (A0) and (A1). For a positive integer N, consider $T^{(N)} = \{Nt : t \in T\}$ and $\widehat{s}_{u_i,T^{(N)}}$ the estimator defined in (11) built on the observation $T^{(N)} \cap E_X(u_i)$, where $u_1, \ldots, u_m$ are fixed. Then, $\sqrt{|T^{(N)}|}(\widehat{s}_{u_1,T^{(N)}} - s_{u_1}, \ldots, \widehat{s}_{u_m,T^{(N)}} - s_{u_m})$ converges in distribution to a centered Gaussian vector with covariance matrix $(\Sigma^2_{s,(u_i,u_j)})_{1\leq i,j\leq m}$, with $\Sigma^2_{s,(u_i,u_j)} = \int_{\mathbb{R}^2} \int_0^{\rho(t)} h_{(u_i,u_j)}(r)\mathrm{d}r\,\mathrm{d}t \in (0,+\infty)$, where*

$$h_{(u_i,u_j)}(r) = \frac{1}{\sqrt{1-r^2}} \exp\left\{\frac{2r s_{u_i} s_{u_j} - r^2 s_{u_i}^2 - r^2 s_{u_j}^2}{2(1-r^2)}\right\}.$$

Proposition 2.1 is a consequence of Proposition A.2 and a multidimensional version of the delta method.

In the sequel we denote by $\sigma^2_{s_u} := \Sigma^2_{s,(u,u)}$ *i.e.*,

$$\sigma^2_{s_u} = \int_{\mathbb{R}^2} \int_0^{\rho(t)} \frac{1}{\sqrt{1-r^2}} \exp\left\{\frac{s_u^2\, r}{1+r}\right\} \mathrm{d}r\,\mathrm{d}t \in (0,+\infty). \tag{13}$$

The function $s_u^2 \mapsto \sigma^2_{s_u}$ is an increasing function, it is minimal when s_u^2 is minimal *i.e.* at $u = \mu$. This leads to the following result.

Corollary 2.1 (Asymptotic variance for $\widehat{s}_{u=\mu,T}$)**.** *Under assumptions of Proposition 2.1, the variance $\sigma^2_{s_u}$ in (13) attains its minimum at $u = \mu$, i.e., $s_u = 0$, and this minimum is*

$$\sigma^2_{s_\mu} = \int_{\mathbb{R}^2} \arcsin(\rho(t))\,\mathrm{d}t.$$

Corollary 2.1 will be useful in Sections 4.1 and 4.2, where we frequently choose the observation level u such that the associated effective level s_u is null. This procedure will guarantee that the estimator has minimal variance.

Proposition 2.2 (Asymptotic normality of $(\widehat{a}_{u_1},\dots,\widehat{a}_{u_m})$)**.** *Let X be a Gaussian random field satisfying Assumptions (A0), (A1) and (A2). Let T_1 and T_2 be two rectangles in T such that $\mathrm{dist}(T_1,T_2)>0$ and $|T_1|=|T_2|>0$. For a positive integer N, let $T_i^{(N)}=\{Nt\,:\,t\in T_i\}$, $i\in\{1,2\}$. Consider $\widehat{a}_{u_i,T^{(N)}}$ the estimator defined in (12) built on the observation $T^{(N)}\cap E_X(u_i)$, $u_i\neq\mu$ being fixed, for $i=1,\dots,m$. Then, $\sqrt{|T_1^{(N)}|}\big(\widehat{a}_{u_1,T^{(N)}}-a,\dots,\widehat{a}_{u_m,T^{(N)}}-a\big)$ converges in distribution to a centered Gaussian vector with covariance matrix $(\Sigma^2_{a,(u_i,u_j)})_{1\le i,j\le m}$ given by*

$$\Sigma^2_{a,(u_i,u_j)}=\frac{(2\pi)^3\left(\Sigma^2_{C_0^*,(u_i,u_j)}+\Sigma^2_{s,(u_i,u_j)}(s_{u_i}^2-1)(s_{u_j}^2-1)C_0^*(X,u_i)C_0^*(X,u_j)\right)}{s_{u_i}^2s_{u_j}^2\exp\{-(\frac{s_{u_i}^2}{2}+\frac{s_{u_j}^2}{2})\}}<+\infty,$$

with $\Sigma^2_{C_0^*,(u_i,u_j)}$ as in Proposition A.1 and $\Sigma^2_{s,(u_i,u_j)}$ as in Proposition 2.1.

Proof of Proposition 2.2 is postponed to Section A.2.

Remark 4. The fact that $\Sigma^2_{C_0^*,(u,u)}$ is nonzero for all levels u still is an open problem. In Estrade and León (2016) the first Itô-Wiener chaos element of the series of $\Sigma^2_{C_0^*,(u,u)}$ has been calculated for all levels u. However, to guarantee that it is nonzero, higher order elements of this series need to be explored. Conversely, the first Itô-Wiener chaos element of the series of $\sigma^2_{C_2^*,u}$ (see, *e.g.*, Müller (2017) and Kratz and Vadlamani (2018)) guarantees it is non degenerate for all $u\in\mathbb{R}$.

Numerical illustrations In the following we provide an illustration of the finite sample performance of the proposed estimator $\widehat{s}_{u,T}$ for several values of u (see Figure 9 in Appendix B). We consider here $M=100$ sample simulations of Gaussian random fields as in Assumption (A0) with $\mu=12$, $\sigma^2=4$ and covariance $r(x)=\mathrm{e}^{-\kappa^2\|x\|^2}$, for $\kappa=100/2^{10}$ in domains of size $2^{10}\times 2^{10}$ pixels.

As expected from Proposition 2.1, the quality of the consistency can be evaluated in the displayed boxplots. Furthermore the associated asymptotic empirical variance is analysed and compared with the theoretical one in the case of $u\mapsto\sigma^2_{s_u}$ in (13) (see right panel in Figure 9 in Appendix B). Furthermore a bias in the estimation of s_u can be observed for values of level u far form μ (see Remark 2). Similar results have been obtained for the estimator of $\widehat{a}_{u,T}$ but they are omitted here for the sake of brevity.

3 Subwindow empirical variance estimation

3.1 Consistent variance estimator

Definition of the subwindow estimators We introduce a technique to estimate the asymptotic variances appearing in Propositions 2.1 and 2.2. Inspired by the cutting of $T^{(N)}$ introduced in Pantle et al. (2010) (see also Bulinski et al. (2012), Section 5) we consider a classical empirical variance estimator. To establish its consistency, we decompose this estimator on domains that are infinitely distant, mimicking the classical context of independent and identically distributed random variables.

Consider the following cutting of $T^{(N)}$: set $M_N\in\mathbb{N}$ such that $M_N\to\infty$ as $N\to\infty$ and consider the grid pattern of $T^{(N)}$ defined by $(V^{(N,(i,j))})_{1\le i,j\le M_N}$- such that $\cup_{1\le i,j\le M_N}V^{(N,(i,j))}=T^{(N)}$, for $(i,j)\neq(i',j')$, $V^{(N,(j,j))}\cap V^{(N,(i',j'))}=\emptyset$ and $|V^{(N,(i,j))}|:=r_N$, $\forall\,1\le i,j\le M_N$ where $r_N\to\infty$ as $N\to\infty$. Observe that, whenever $\max\{|i-i'|,|j-j'|\}\ge 2$ then $\mathrm{dist}(V^{(N,(i,j))},V^{(N,(i',j'))})\to\infty$ as $N\to\infty$. Then, by Propositions A.1 and A.2 the estimators $\widehat{C}_\ell^{\,\prime V^{(N,(i,j))}}(X,u)$, for $\ell\in\{0,2\}$, are consistent and

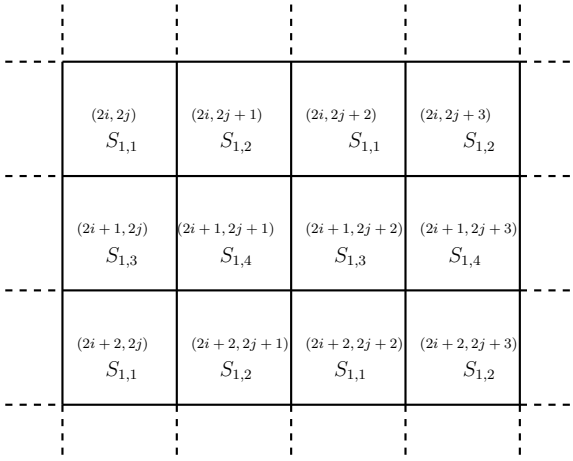

Figure 1: Decomposition of the sum S_1 in (15) in four sums.

asymptotically independent. Therefore, we estimate the asymptotic variances appearing in Propositions A.1 and A.2 by

$$\widehat{\Sigma}^2_{C^*_\ell,(u,v)} = \frac{1}{M_N^2-1}\sum_{i,j=1}^{M_N} \widehat{\xi}_N^{(i,j)}(u)\widehat{\xi}_N^{(i,j)}(v) - \Big(\frac{1}{M_N^2-1}\sum_{i,j=1}^{M_N} \widehat{\xi}_N^{(i,j)}(u)\Big)\Big(\frac{1}{M_N^2-1}\sum_{i,j=1}^{M_N} \widehat{\xi}_N^{(i,j)}(v)\Big), \tag{14}$$

where we define $\widehat{\xi}_N^{(i,j)}(u) := \widehat{C}_\ell^{/V^{(N,(i,j))}}(X,u)$, for all $u \in \mathbb{R}$, $\ell \in \{0,2\}$, $1 \le i,j \le M_N$. The key point is that these estimators are identically distributed, as the field X is stationary, and are asymptotically independent whenever $\max\{|i-i'|,|j-j'|\} \ge 2$ in view of Propositions A.1 and A.2 and the fact that $\mathrm{dist}(V^{(N,(i,j))}, V^{(N,(i',j'))}) \to \infty$, as $N \to \infty$.

Case of the area ($\ell = 2$ in Equation (14)) To the knowledge of the authors, the only result establishing the consistency of (14), is Theorem 6 of Bulinski et al. (2012) in the case of the area ($\ell = 2$). However, this results imposes a condition (39) on the fourth-order cumulent that is difficult to check and for which the example provided is "a random field X with finite dependence range", which means that $\rho = \rho \mathbf{1}_D$ for some finite domain D. In the following Theorem 3.1 we prove consistency of the estimator $\widehat{\Sigma}^2_{C^*_2,(u,v)}$ defined in (14) under Assumption ($\mathcal{A}1$).

Theorem 3.1. *Let X a Gaussian random field satisfying Assumptions ($\mathcal{A}0$) and ($\mathcal{A}1$). Let $\widehat{\Sigma}^2_{C^*_2,(u_q,u_k)}$ as in (14) with $q,k \in \{1,\dots,m\}$. Then, it holds that $\widehat{\Sigma}^2_{C^*_2,(u_q,u_k)} \xrightarrow[N\to\infty]{\mathbb{P}} \Sigma^2_{C^*_2,(u_q,u_k)}$.*

Proof of Theorem 3.1. We show the consistency of estimators $\widehat{\Sigma}^2_{C^*_2,(u_q,u_k)}$ in (14), for all $q,k \in \{1,\dots,m\}$. First, note that $\widehat{\Sigma}^2_{C^*_2,(u_q,u_k)}$ is given by the difference of two terms, write

$$\widehat{\Sigma}^2_{C^*_2,(u_q,u_k)} := S_1(u,v) - S_2(u)S_2(v). \tag{15}$$

By Proposition 2.1 and the additivity of $T \mapsto C_2^{/T}(X,u)$, we get that for all u, $S_2(u) \xrightarrow[N\to\infty]{\mathbb{P}} C_2^*(X,u)$. The remaining of the proof consists is noticing that the sum S_1 can be rewritten as four sums each composed of identically distributed terms that are asymptotically independent. Decompose S_1 as follows

(see Figure 1) and without loss of generality assume that M_N is even, then

$$\begin{aligned}S_1 &= \frac{1}{M_N^2-1}\sum_{i,j=1}^{M_N}\widehat{\xi}_N^{(2i,2j)}(u_q)\widehat{\xi}_N^{(2i,2j)}(u_k) + \frac{1}{M_N^2-1}\sum_{i,j=1}^{M_N}\widehat{\xi}_N^{(2i,2j+1)}(u_q)\widehat{\xi}_N^{(2i,2j+1)}(u_k)\\ &+ \frac{1}{M_N^2-1}\sum_{i,j=1}^{M_N}\widehat{\xi}_N^{(2i+1,2j)}(u_q)\widehat{\xi}_N^{(2i+1,2j)}(u_k) + \frac{1}{M_N^2-1}\sum_{i,j=1}^{M_N}\widehat{\xi}_N^{(2i+1,2j+1)}(u_q)\widehat{\xi}_N^{(2i+1,2j+1)}(u_k)\\ &:= S_{1,1}+S_{1,2}+S_{1,3}+S_{1,4}.\end{aligned}$$

To show that $S_{1,p} - \frac{1}{4}\mathbb{E}[\widehat{\xi}_N^{(1,1)}(u)\widehat{\xi}_N^{(1,1)}(v)] \xrightarrow[N\to\infty]{\mathbb{P}} 0$, $1\le p\le 4$, we show that the convergence holds in L_2. We perform computations for $S_{1,1}$, other sums are treated similarly. It holds, using the stationarity of the field, that

$$\begin{aligned}\mathbb{V}(S_{1,1}) &= \frac{1}{(M_N^2-1)^2}\sum_{i,i',j,j'=1}^{M_N}\mathrm{Cov}\big(\widehat{\xi}_N^{(2i,2j)}(u_q)\widehat{\xi}_N^{(2i,2j)}(u_k), \widehat{\xi}_N^{(2i',2j')}(u_q)\widehat{\xi}_N^{(2i',2j')}(u_k)\big)\\ &= \frac{1}{(M_N^2-1)^2}\sum_{(i,j)\neq(i',j')=1}^{M_N}\mathrm{Cov}\big(\widehat{\xi}_N^{(2i,2j)}(u_q)\widehat{\xi}_N^{(2i,2j)}(u_k), \widehat{\xi}_N^{(2i',2j')}(u_q)\widehat{\xi}_N^{(2i',2j')}(u_k)\big) \qquad (16)\\ &+ \frac{1}{(M_N^2-1)^2}\sum_{i,j=1}^{M_N}\mathrm{Cov}\big(\widehat{\xi}_N^{(2i,2j)}(u_q)\widehat{\xi}_N^{(2i,2j)}(u_k), \widehat{\xi}_N^{(2i,2j)}(u_q)\widehat{\xi}_N^{(2i,2j)}(u_k)\big). \qquad (17)\end{aligned}$$

For all $(i,j)\in\{1,\dots,M_N\}^2$, if we set $G=(X-\mu)/\sigma$ it holds that

$$\widehat{\xi}_N^{(i,j)}(u) = \widehat{C}_2^{/V^{(N,(i,j))}}(X,u) = \widehat{C}_2^{/V^{(N,(i,j))}}(G,s_u) = \frac{\mathcal{L}_2(G,s_u,V^{(N,(i,j))})}{|V^{(N,(i,j))}|}.$$

The remaining of the proof is a direct consequence of the following result.

Proposition 3.1. *Let X be a Gaussian random field satisfying Assumptions (A0) and (A1) and set $G=(X-\mu)/\sigma$. Let u_1,u_2,u_3,u_4 four fixed levels in $\mathbb{R}$ and associated* effective levels *$s_{u_i}=(u_i-\mu)/\sigma$, for $i\in\{1,2,3,4\}$. Let T and T' be such that $|T|=|T'|$ and $\mathrm{dist}(T,T')\to\infty$. Then, it holds that,*

$$\mathbb{E}[\mathcal{L}_2(G,s_{u_1},T)\mathcal{L}_2(G,s_{u_2},T)\mathcal{L}_2(G,s_{u_3},T')\mathcal{L}_2(G,s_{u_4},T')] = \psi(s_{u_1})\psi(s_{u_2})\psi(s_{u_3})\psi(s_{u_4})|T|^4 + o(|T|^3).$$

Proof of Proposition 3.1 is postponed to Section A.3. Proposition 3.1 ensures that (16) goes to 0. Let $(i,j)\neq(i',j')\in\{1,\dots,M_N\}^4$ and $T=V^{(N,(i,j))}$ and $T'=V^{(N,(i',j'))}$, for which for N large enough it holds $\mathrm{dist}(V^{(N,(i,j))},V^{(N,(i',j'))})>1$ and $|V^{(N,(i,j))}|=|V^{(N,(i',j'))}|\to\infty$ as $N\to\infty$, then we derive

$$\lim_{n\to\infty}\mathrm{Cov}\big(\widehat{\xi}_N^{(2i,2j)}(u_q)\widehat{\xi}_N^{(2i,2j)}(u_k), \widehat{\xi}_N^{(2i',2j')}(u_q)\widehat{\xi}_N^{(2i',2j')}(u_k)\big) = 0.$$

This implies that (16) goes to 0 as $N\to\infty$ using Cesàro Lemma. Moreover, Equation (17) vanishes using that $|\widehat{\xi}_N|\le 1$ alsmost surely, implying (17) is bounded by $M_N^2/(M_N^2-1)^2\to 0$, as $N\to\infty$. This implies that $\mathbb{V}(S_{1,1})\to 0$ as $N\to\infty$ using Cesàro Lemma. The same behaviour holds true for $\mathbb{V}(S_{1,p})$ for all $p\in\{1,2,3,4\}$, implying the desired result in Theorem 3.1. □

Discussion Theorem 3.1 establishes consistency of this subwindow variance estimator in the case of the area under Assumption ($\mathcal{A}1$). This assumption seems weak as it is the same assumption as the one imposed to get the asymptotic normality of $\widehat{C}_2(X,u)$ (see Theorem 4 of Bulinski et al. (2012)).

Establishing Theorem 3.1 is more difficult than it may seem; since the quantities $(\widehat{\xi}_N^{(i,j)})_{i,j}$ depend on the asymptotic N, we cannot apply ergodic theorems. Moreover, no inequality permits to upper bound the covariance between the $(\widehat{\xi}_N^{(i,j)})_{i,j}$ by a function the covariance function ρ of the field, which would lead to more direct arguments.

A key element in the proof of Theorem 3.1 is Proposition 3.1 which is similar to the constraint (39) of Bulinski et al. (2012). More precisely, in Proposition 3.1 we control covariances terms between distant domains. Proof of Proposition 3.1 relies on two ingredients: *i.* the Itô-Wiener chaos decomposition of $\mathcal{L}_2(X,u,T)$ and *ii.* the diagram formula (see Taqqu (1977), Lemma 3.2) applied up to the dimension 4. This diagram formula in dimensions 3 and 4 yields to technical and lengthly computations where the constraint $\mathrm{dist}(V^{(N,(i,j))}, V^{(N,(i',j'))}) \to \infty$ as $N \to \infty$, and the cutting of $T^{(N)}$, plays a crucial part.

In the result below, we provide a direct consequence of Theorem 3.1: the consistency of the estimator for $\Sigma^2_{s,(u_i,u_j)}$, introduced in Proposition 2.1.

Corollary 3.1. *Let X a Gaussian random field satisfying Assumptions ($\mathcal{A}0$) and ($\mathcal{A}1$). Define, the estimator of $\Sigma^2_{s,(u_i,u_k)}$, where $(i,k) \in \{1,\dots,m\}^2$, by*

$$\widehat{\Sigma}^2_{s,(u_i,u_k)} = 2\pi \exp\left\{\frac{1}{2}(\widehat{s}^2_{u_i} + \widehat{s}^2_{u_k})\right\} \widehat{\Sigma}^2_{C_2^*,(u_i,u_k)}, \tag{18}$$

with $\widehat{s}_u := \widehat{s}_{u,T^{(N)}}$ as in Proposition 2.1. Then, it holds that, for $(i,k) \in \{1,\dots,m\}^2$,

$$\widehat{\Sigma}^2_{s,(u_i,u_k)} \xrightarrow[N\to\infty]{\mathbb{P}} \Sigma^2_{s,(u_i,u_k)}.$$

Case of the Euler characteristic ($\ell = 0$ in Equation (14)) In the case of the Euler characteristic ($\ell = 0$), the same proof should generalize under the following additional assumption.

($\mathcal{A}3$) Suppose that Assumption ($\mathcal{A}2$) holds true with $|M_r(t)| \le C_M/(1+\|t\|)^\gamma$ where C_M is a positive constant and $\gamma > 2$.

Indeed there is a Itô-Wiener chaos decomposition of $\mathcal{L}_0(X,u,T)$ (see Section A.4) with similar properties on the coefficients. However, computing the fourth moment with this chaos decomposition would imply to use the diagram formula in dimensions 18 and 24, which become extremely technical and burdensome. Therefore, we give in Appendix A.4 some ingredients to establish the following Conjecture 3.1 which is an equivalent of Proposition 3.1 in the case of the Euler characteristic having for all $(i,j) \in \{1,\dots,M_N\}^2$,

$$\widehat{\xi}_N^{(i,j)}(u) = \widehat{C}_0^{/V^{(N,(i,j))}}(X,u) = \frac{\mathcal{L}_0(X,u,V^{(N,(i,j))})}{|V^{(N,(i,j))}|}.$$

The missing step in the proof to have the result is the computation of the diagram formula in dimensions 18 and 24.

Conjecture 3.1. *Let X a Gaussian random field satisfying Assumptions ($\mathcal{A}0$) and ($\mathcal{A}3$). Let T and T' be such that $|T| = |T'|$ and $\mathrm{dist}(T,T') \to \infty$. Let u_1,u_2,u_3,u_4 four fixed levels in $\mathbb{R}$. Then it holds that*

$$\begin{aligned}&\mathbb{E}[\mathcal{L}_0(X,u_1,T)\mathcal{L}_0(X,u_2,T)\mathcal{L}_0(X,u_3,T')\mathcal{L}_0(X,u_4,T')] \\ &\qquad = \frac{a^4}{(2\pi)^6}\exp\{-\frac{1}{2}(s^2_{u_1}+s^2_{u_2}+s^2_{u_3}+s^2_{u_4})\}s_{u_1}s_{u_2}s_{u_3}s_{u_4}|T|^4 + o(|T|^4),\end{aligned}$$

where a denotes the effective spectral moment of X in Definition 1.2.

Mimicking the proof of Theorem 3.1, we derive that a consequence of Conjecture 3.1 is that

$$\widehat{\Sigma}^2_{C_0^*,(u_q,u_k)} \xrightarrow[N\to\infty]{\mathbb{P}} \Sigma^2_{C_0^*,(u_q,u_k)}. \tag{Conjecture}$$

Then, using (Conjecture), one can conjecture the consistency of the estimator for $\Sigma^2_{a,(u_i,u_j)}$, introduced in Proposition 2.2.

Conjecture 3.2. *Let X a Gaussian random field satisfying Assumptions (A0), (A1) and (A3). Define the estimator of $\Sigma^2_{a,(u_i,u_k)}$, where $(i,k) \in \{1,\dots,m\}^2$,*

$$\widehat{\Sigma}^2_{a,(u_i,u_k)} = \frac{(2\pi)^3 \left(\widehat{\Sigma}^2_{C_0^*,(u_i,u_k)} + \widehat{\Sigma}^2_{s,(u_i,u_k)}(\widehat{s}^2_{u_i}-1)(\widehat{s}^2_{u_k}-1)\widehat{C}_{0,T^{(N)}}(X,u_i)\widehat{C}_{0,T^{(N)}}(X,u_k)\right)}{\widehat{s}^2_{u_i}\widehat{s}^2_{u_k}\exp\left\{-\left(\frac{\widehat{s}^2_{u_i}}{2}+\frac{\widehat{s}^2_{u_k}}{2}\right)\right\}},$$

with $\widehat{s}_u := \widehat{s}_{u,T^{(N)}}$ as in Proposition 2.1, $\widehat{\Sigma}^2_{s,(u_i,u_k)}$ as in (18) and $\widehat{C}_{0,T^{(N)}}(X,u_k)$ as in (10). Then,

$$\widehat{\Sigma}^2_{a,(u_i,u_k)} \xrightarrow[N\to\infty]{\mathbb{P}} \Sigma^2_{a,(u_i,u_k)}.$$

3.2 Statistical implications and numerical illustrations

In this section we consider several useful applications of theoretical results provided in Sections 2 and 3.1. Indeed, the asymptotically Gaussian estimators of the unknown location and scale parameters and the subwindow empirical variance estimators are used in the following to build a test of Gaussianity using LK densities (see Section 3.2.1). An asymptotic interval for the unknown location μ is given in Section 3.2.2.

3.2.1 A Gaussianity test for non standard fields

Here we generalize the test of Biermé et al. (2019) in cases where the field is not supposed to be centered and with unit variance. We test the assumption

$$H_0 \ : X \text{ is Gaussian field with unknown mean and unknown variance,}$$

where X is a Gaussian field satisfying Assumptions (A0) and (A2). Consider the quantities

$$R(u_1,u_2) := \frac{C_0^*(X,u_2)}{C_0^*(X,u_1)} \overset{\text{under } H_0}{=} \frac{s_{u_2}}{s_{u_1}}\exp\{-\frac{1}{2}(s^2_{u_2}-s^2_{u_1})\} := R^{H_0}(u_1,u_2).$$

This ratio is empirically accessible provided the field is observed at two distinct levels u_1 and u_2,

$$\widehat{R}_T(u_1,u_2) := \frac{\widehat{C}_{0,T}(X,u_2)}{\widehat{C}_{0,T}(X,u_1)}. \tag{19}$$

We establish below a central limit theorem for $\widehat{R}_T(u_1,u_2)$. Notice that one can readily establish a CLT for $\sqrt{|T|}\left(\widehat{R}_T(u_1,u_2) - R^{H_0}(u_1,u_2)\right)$ using, for instance, Proposition A.1, but as $R^{H_0}(u_1,u_2)$ is unknown, this CLT does not allow to determine a rejection level. Define

$$\widehat{R}^{H_0}_T(u_1,u_2) := \frac{\widehat{s}_{u_2}}{\widehat{s}_{u_1}}\exp\left\{-\frac{1}{2}\left(\widehat{s}^2_{u_2}-\widehat{s}^2_{u_1}\right)\right\}. \tag{20}$$

For technical reasons, we estimate $\widehat{R}_{T_1}(u_1,u_2)$ and $\widehat{R}^{H_0}_{T_2}(u_2,u_1)$ on rectangles T_1 and T_2 that are asymptotically infinitely distant so that both excursion sets are asymptotically independent and lead to independent estimators.

Proposition 3.2. *Assume that X is a Gaussian field satisfying Assumptions (A0), (A1) and (A2). Let $u_1, u_2 \neq \mu$ being fixed. Let T_1 and T_2 be two rectangles in $\mathbb{R}^2$ such that dist$(T_1, T_2) > 0$ and $|T_1| = |T_2| > 0$. For any positive integer N, we define $T_i^{(N)} = \{Nt : t \in T_i\}$, for $i = 1, 2$. Then, under H_0 it holds that*

$$\sqrt{|T_1^{(N)}|}\big(\widehat{R}_{T_1^{(N)}}(u_1,u_2) - \widehat{R}^{H_0}_{T_2^{(N)}}(u_1,u_2)\big) \xrightarrow[N\to\infty]{d} \mathcal{N}(0, \sigma^2_{R_{u_1,u_2}}),$$

where $\sigma^2_{R_{u_1,u_2}} < \infty$ and $\widehat{R}_{T_1}(u_1,u_2)$ (resp. $\widehat{R}^{H_0}_2(u_1,u_2)$) is defined as in (19) (resp. in (20)) built on the observation $T_1^{(N)} \cap E_X(u_1)$ and $T_1^{(N)} \cap E_X(u_2)$ (resp. $T_2^{(N)} \cap E_X(u_1)$ and $T_2^{(N)} \cap E_X(u_2)$).

Proof of Proposition 3.2 is postponed to Section A.2.

Subwindow empirical estimation of variance $\sigma^2_{R_{u_1,u_2}}$ We provide a normalized version of Proposition 3.2, we built a consistent estimator for $\sigma^2_{R_{u_1,u_2}}$, *i.e.*,

$$\widehat{\sigma}^2_{R_{u_1,u_2}} = \widehat{\sigma}^2_{g(C_0^*),(u_1,u_2)} + \widehat{\sigma}^2_{h(s),(u_1,u_2)} := \widehat{\mathbb{V}}(\widehat{R}_{T_1^{(N)}}(u_1,u_2))\,|T_1^{(N)}| + \widehat{\mathbb{V}}(\widehat{R}^{H_0}_{T_2^{(N)}}(u_1,u_2))\,|T_2^{(N)}|. \tag{21}$$

Consistent estimators for $\mathbb{V}(\widehat{R}_{T^{(N)}}(u_1,u_2))$ and $\mathbb{V}(\widehat{R}^{H_0}_{T^{(N)}}(u_1,u_2))$ are obtained using the subwindows technique of Section 3.1. Define $\widehat{\sigma}^2_{h(s),(u_1,u_2)}$ in (21) by

$$\widehat{\sigma}^2_{h(s),(u_1,u_2)} = \mathrm{e}^{-(\widehat{s}^2_{u_2} - \widehat{s}^2_{u_1})}\Big[\widehat{\sigma}^2_{s_{u_2}}\Big(\tfrac{1-\widehat{s}^2_{u_2}}{\widehat{s}_{u_1}}\Big)^2 + 2\,\widehat{\Sigma}^2_{s,(u_1,u_2)}\Big(\tfrac{1-\widehat{s}^2_{u_2}}{\widehat{s}_{u_1}}\Big)\Big(\widehat{s}_{u_2} - \tfrac{\widehat{s}_{u_2}}{\widehat{s}^2_{u_1}}\Big) + \widehat{\sigma}^2_{s_{u_1}}\Big(\widehat{s}_{u_2} - \tfrac{\widehat{s}_{u_2}}{\widehat{s}_{u_1}}^2\Big)^2\Big],$$

with $\widehat{s}_{u_i} := \widehat{s}^2_{u_i,T_2^{(N)}}$ defined in (11) , $\widehat{\Sigma}^2_{s,(u_1,u_2)}$ and $\widehat{\sigma}^2_{s_{u_i}}$ as in Corollary 3.1. From Proposition 2.1 and Corollary 3.1, it holds that $\widehat{\sigma}^2_{h(s),(u_1,u_2)} \xrightarrow[N\to\infty]{\mathbb{P}} \sigma^2_{h(s),(u_1,u_2)}$. Similarly, define $\widehat{\sigma}^2_{g(C_0^*),(u_1,u_2)}$

$$\widehat{\sigma}^2_{g(C_0^*),(u_1,u_2)} = \frac{\widehat{\sigma}^2_{C_0^*,u_2}}{\widehat{C}_{0,T_1^{(N)}}(X,u_1)^2} - 2\frac{\widehat{C}_{0,T_1^{(N)}}(X,u_2)}{\widehat{C}_{0,T_1^{(N)}}(X,u_1)^3}\widehat{\Sigma}^2_{C_0^*,(u_1,u_2)} + \frac{\widehat{C}_{0,T_1^{(N)}}(X,u_2)^2}{\widehat{C}_{0,T_1^{(N)}}(X,u_1)^4}\widehat{\sigma}^2_{C_0^*,u_1},$$

with $\widehat{C}_{0,T_1^{(N)}}(X,u_i)$ as in (10) and $\widehat{\Sigma}^2_{C_0^*,(u_1,u_2)}$ as in (Conjecture).

Take a confidence level $\alpha \in (0,1)$ and set $q_{1-\frac{\alpha}{2}}$ such that $\mathbb{P}(|N(0,1)| \leq q_{1-\frac{\alpha}{2}}) = 1 - \frac{\alpha}{2}$. We define the symmetric test $\phi_{T^{(N)}}$ with asymptotic level α as

$$\phi_{T_1^{(N)},T_2^{(N)}} = \mathbf{1}\left\{\sqrt{\frac{|T_1^{(N)}|}{\widehat{\sigma}^2_{R_{u_1,u_2}}}}\left|\widehat{R}_{T_1^{(N)}}(u_1,u_2) - \widehat{R}^{H_0}_{T_2^{(N)}}(u_1,u_2)\right| \geq q_{1-\frac{\alpha}{2}}\right\},$$

where $\widehat{\sigma}^2_{R_{u_1,u_2}}$ is the consistent variance estimator built before.

Comments The test statistics is well define for all level $u \neq \mu$, similarly to Biermé et al. (2019) where we could not use the level $u = 0$. Here μ is unknown and choosing u_1 close to μ will make the ratio $\widehat{R}_T(u_1,u_2)$ unstable. A solution is to modify the test statistics and consider the difference $\widetilde{R}_T(u_1,u_2) = \widehat{C}_{0,T}(X,u_2) - \widehat{C}_{0,T}(X,u_1)$ instead. The test could be modified accordingly at the expense of more tedious calculations, in particular due to the fact that the unknown quantity $a := \frac{\lambda}{\sigma^2}$ will appear in the test statistics $\widetilde{R}_T(u_1,u_2)$ under H_0.

Furthermore, under H_0 we do not impose any constraint on the shape of the covariance function nor on the spectral moment other than Assumptions ($\mathcal{A}1$) and ($\mathcal{A}2$). In particular, the spectral moments of X under H_0 and the alternative hypothesis can be different. However, contrary to the case where the field is centered with unit variance (see Biermé et al. (2019)), the test statistic under H_0 depends on unknown quantities (μ, σ^2).

3.2.2 Asymptotic interval for μ

We propose the following construction for an interval containing the unknown location μ of the field based on the observations $T \cap E_X(u_1)$, for J fixed levels $u_1 < \ldots < u_J$.

Procedure to build interval for the unknown location of the field

Input :

Let $J \in \mathbb{N}$ be fixed, the field X is observed at levels $u_1 < \ldots < u_J$.

Estimation :

Let $\widehat{\sigma}^2_{s_{u_j}} := \widehat{\Sigma}^2_{s,(u_i,u_i)}$, with $j \in \{1, \ldots, J\}$ and $\widehat{\Sigma}^2_{s,(u_i,u_i)}$ as in (18).

Define $\widehat{j} = \underset{j\in\{1,\ldots,J\}}{\operatorname{argmin}} \widehat{\sigma}^2_{s_{u_j}}$ and

$$\widehat{j}^{\pm 1} = \begin{cases} \widehat{j}+1 & \text{if } \widehat{\sigma}^2_{s_{u_{\widehat{j}+1}}} \leq \widehat{\sigma}^2_{s_{u_{\widehat{j}-1}}} \\ \widehat{j}-1 & \text{if } \widehat{\sigma}^2_{s_{u_{\widehat{j}-1}}} \leq \widehat{\sigma}^2_{s_{u_{\widehat{j}+1}}} \end{cases},$$

Final output :

The following interval contains μ with large probability: $I_\mu := \left[\min\{u_{\widehat{j}}, u_{\widehat{j}^{\pm 1}}\}, \max\{u_{\widehat{j}}, u_{\widehat{j}^{\pm 1}}\}\right]$

with convention that if $\widehat{j} = 0$, $I_\mu := [-u_1, u_0]$ and if $\widehat{j} = J$, $I_\mu := [u_J, -u_{J-1}]$.

Proposition 3.3. *It holds that* $\mathbb{P}\big(\mu \in \left[\min\{u_{\widehat{j}}, u_{\widehat{j}^{\pm 1}}\}, \max\{u_{\widehat{j}}, u_{\widehat{j}^{\pm 1}}\}\right]\big) \underset{T \nearrow \mathbb{R}^2}{\longrightarrow} 1.$

Proof of Proposition 3.3 is postponed to Section A.2.

4 Test to compare two images of excursion sets

Let Y and Z be two stationary Gaussian fields satisfying Assumptions ($\mathcal{A}0$) and ($\mathcal{A}1$) with possibly different mean, variance, spectral moment or correlation function. Suppose one has two images of the excursion sets of these fields observed at the respective levels u_Y and u_Z and wants to know if it is possible to compare the Lipshitz-Killing curvatures of theses two images, *i.e.* one want to test whether the *effective level* of Y (denoted by $s_{u_Y}(Y)$) is equal to the *effective level* of Z (denoted by $s_{u_Z}(Z)$):

$$H_0 \,:\, s_{u_Y}(Y) = s_{u_Z}(Z) \qquad H_1 \,:\, s_{u_Y}(Y) \neq s_{u_Z}(Z).$$

Introduce the quantity $S(Y,Z) := s_{u_Y} - s_{u_Z}$ and $\widehat{S}_{T^{(N)}}(Y,Z) := \widehat{s}_{u_Y,T^{(N)}} - \widehat{s}_{u_Z,T^{(N)}}$ its empirical counterpart. Notice that $S(Y,Z) = 0$ under the null hypothesis. We can now state the auto-normalised central limit theorem for the test statistics $\widehat{S}_{T^{(N)}}(Y,Z)$.

Corollary 4.1. *Let X be a Gaussian random field satisfying Assumptions (A0) and (A1). It holds that*

$$\sqrt{\frac{1}{\widehat{\Sigma}_{Y,Z}}}\,\widehat{S}_{T^{(N)}}(Y,Z) \xrightarrow[N\to\infty]{d,\,H_0} \mathcal{N}(0,1), \qquad \textit{where} \qquad \widehat{\Sigma}_{Y,Z} = \widehat{\sigma}^2_{s,u_Y} + \widehat{\sigma}^2_{s,u_Z},$$

*with $\widehat{\sigma}^2_{s,u_Y} := \widehat{\Sigma}^2_{s,(u_Y,u_Y)}$ (*resp. *$\widehat{\sigma}^2_{s,u_Z} := \widehat{\Sigma}^2_{s,(u_Z,u_Z)}$), the consistent estimator of the variance in (18).*

Corollary 4.1 is proved by using Proposition 2.1, Corollary 3.1 and Theorem 3.1. Notice that due to the independence of the two consider images, we get a simplified expression for the asymptotic variance.

Let $q_{1-\frac{\alpha}{2}}$ such that $\mathbb{P}(|N(0,1)| \leq q_{1-\frac{\alpha}{2}}) = 1 - \frac{\alpha}{2}$. Finally, we introduce the symmetric test $\phi_{T^{(N)}}$ with asymptotic level α:

$$\phi_{T^{(N)}} = \mathbf{1}_{\left\{\sqrt{\frac{1}{\widehat{\Sigma}_{Y,Z}}}\left|\widehat{S}_{T^{(N)}}(Y,Z)\right| \geq q_{1-\frac{\alpha}{2}}\right\}}. \tag{22}$$

In the following, we evaluate the performances of the proposed test $\phi_{T^{(N)}}$ in (22) on simulated mammograms (from a digital texture model, see Section 4.1) and on real mammograms (from mini-MIAS database, see Section 4.2). In particular, we aim to test whether the *effective level* of an image is equal to the *effective level* of another one.

4.1 Comparing images of excursion sets: a synthetic mammograms study

The data-set In this section we consider images from a recent solid breast texture model inspired by the morphology of medium and small scale fibro-glandular and adipose tissue observed in clinical breast computed tomography (bCT) images (UC Davis database). Each adipose compartment is modeled as a union of overlapping ellipsoids and the underlying dynamic is dictated by a spatial marked point process. The contour of each ellipsoid is blurred to render the model more realistic (for details see Li et al. (2016), Section 2.2 and Figure 1). Finally, the synthetic mammograms images were simulated by x-ray projection. Evaluation provided in Li et al. (2016) has shown that simulated mammograms and digital breast tomosynthesis images are visually similar, according to medical experts.

We consider 15 simulated 2D images generated by this texture model. The images were kindly provided by GE Healthcare France, department *Mammography*. From a clinical point of view, radiologists use the Breast Imaging Reporting and Data System (or BI-RADS) to classify breast density into four categories. They go from almost all fatty tissue to extremely dense tissue with very little fat. In this latter category, it can be hard to see small tumors in or around the dense tissue. The images we studied belong to three morphologic situation groups :

(F) Almost entirely adipose breasts;

(FG) Scattered fibro-glandular dense breasts;

(D) Heterogeneously dense breasts.

The first image from each group is reported in Figure 2. As observed in Section 3 in Li et al. (2016), these simulated digital mammograms from groups (F), (FG) and (D) show a high visual realism compared to real images in these 3 different clinical situations (see also Figure 5).

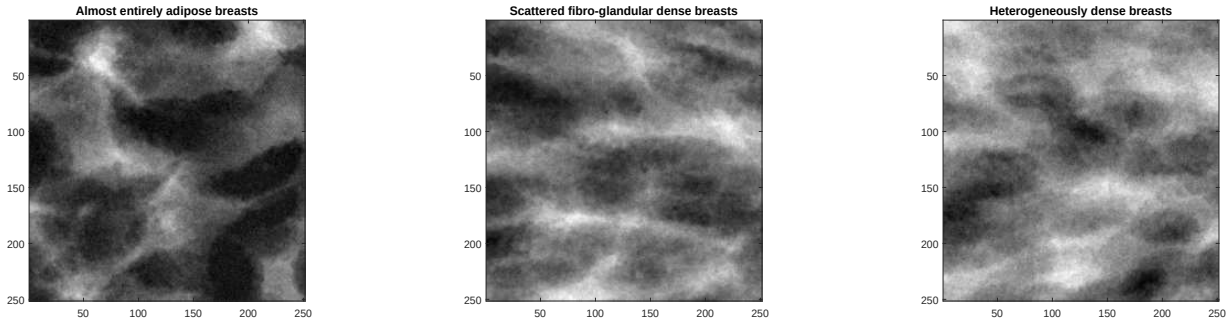

Figure 2: Synthetic digital mammograms study. Image 1.F from group (F) (left), 1.FG from group (FG) (center) and 1.D from group (D) (right). Image size: 251×251.

Importance of the *effective level* In Figure 3 (left) we estimate the *effective levels* $\widehat{s}_u$ for different values of u. One can appreciate that the estimated *effective levels* are different for each group of mammograms. Moreover, it seems there exists an order between the three groups of mammograms in terms of *effective levels*. This means that if one want to compare images from different groups, one cannot use the same value of u to perform the comparison. Indeed, in Figure 3 (right-up) we display the excursion sets of the first image of each groups (denoted image 1.F, 1.FG and 1.D in Figure 2) for the same fixed level $u = 2200$. The resulting excursion sets look completely different from one group to the other. However this difference is not necessarily the result of a intrinsic difference between the images, but a problem in the calibration of the level u used for the comparison. On this example, as we observed in Figure 3 (left) a difference between the groups of *effective levels*, we calibrate a level u for each group such that they all have an *effective level* close to 0, *i.e.*, adaptive levels $\widetilde{u}$, such that $|\widehat{s}_{\widetilde{u}}| < \epsilon$, for $\epsilon = 10^{-2}$. Notice that this choice guarantees a minimal variance for the estimated *effectively level* (see Corollary 2.1). Figure 3 (right-down) is obtained by considering $\widetilde{u}_{1.F} = 2133$, $\widetilde{u}_{1.FG} = 2291$, $\widetilde{u}_{1.D} = 2518$.

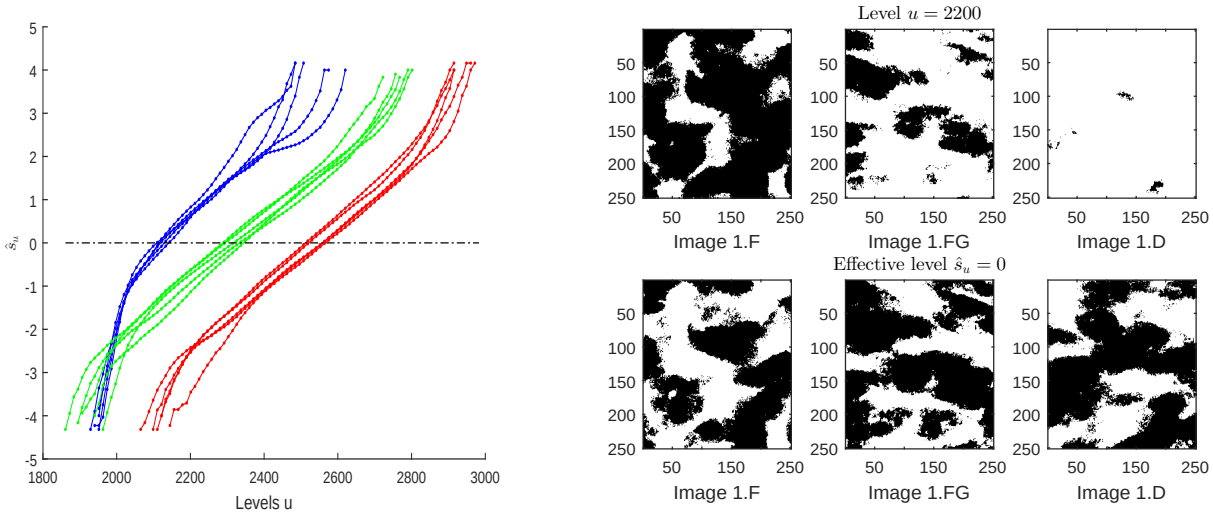

Figure 3: Synthetic digital mammograms study. **Left**: Estimated $\widehat{s}_u$ for several values of u for each image: group (F) in blue curves, (FG) in green curves and (D) in red ones. **Right**: Excursion sets for a fixed level $u = 2200$ (first row) and for the three adaptive levels $\widetilde{u}$, such that for each $\widetilde{u}$ it holds that $|\widehat{s}_{\widetilde{u}}| < \epsilon$, for $\epsilon = 10^{-2}$ (second row).

We observe now that the excursion sets in Figure 3 (right-down) look visually similar. Moreover, at these levels $\widetilde{u}$, we theoretically expect to get estimated Euler characteristic values close to zero (see Equation (7)). This behavior is illustrated in the boxplots gathered in Figure 10 in Appendix B. Then, any geometric estimated quantity (as for instance the Lipshitz-Killing curvatures) on these excursion sets cannot be compared at the same levels but at the same *effective levels*.

Testing two images of excursion sets We now test for the 1.F, 1.FG, 1.D images in Figure 2:

$$H_0 \,:\, s_{\widetilde{u}_Y}(Y) = s_{\widetilde{u}_Z}(Z) \qquad \text{versus} \qquad H_1 \,:\, s_{\widetilde{u}_Y}(Y) \neq s_{\widetilde{u}_Z}(Z), \tag{23}$$

for $Y, Z \in \{$1.F,1.FG, 1.D$\}$, where $\widetilde{u}_Y$ and $\widetilde{u}_Z$ are the adaptive levels previously defined and such that $|\widehat{s}_{\widetilde{u}}| < 10^{-2}$, *i.e.*, the associated $\widehat{C}_{0,T}(\widetilde{u})$ is zero (see right panel of Figure 3 and boxplots in Figure 10).

Indeed, for these levels $\widetilde{u}_{1.F}$, $\widetilde{u}_{1.FG}$, $\widetilde{u}_{1.D}$, the $p-$values of the test (23), gathered in Table 1 below, lead to accept the H_0 hypothesis. This preliminary adjustment of the image level is necessary to properly compare the excursion sets. In case only two excursion sets are available and not the whole images, this test (23) can be a preliminary prerequisite to determine whether or not it is legitimate to perform a comparison between these images.

1.F versus 1.FG	1.F versus 1.D	1.FG versus 1.D
0.9858	0.9511	0.9642

Table 1: Synthetic digital mammograms study. $p-$values associated to the test $H_0 \,:\, s_{\widetilde{u}_Y}(Y) = s_{\widetilde{u}_Z}(Z)$ for excursion sets in Figure 3 (right, second row) with $\widetilde{u}_{1.F} = 2133$, $\widetilde{u}_{1.FG} = 2291$, $\widetilde{u}_{1.D} = 2518$.

We now consider 1000 different values of u and for each u we perform the following test

$$H_0 \,:\, s_u(Y) = s_u(Z) \qquad \text{versus} \qquad H_1 \,:\, s_u(Y) \neq s_u(Z), \tag{24}$$

for Y, Z images of this synthetic mammograms data-set. Notice that, contrary to the test (23), we did not previously choose adaptive levels. Then the test (24) is performed for possible different *effective levels* s_u. In Table 2 we display the number of $p-$values associated to the 1000 values of u that are smaller than the significant level $\alpha = 0.2$. In particular we perform an intra-class analysis (left panel in Table 2 in Appendix B) and an inter-classes analysis (right panel in Table 2 in Appendix B).

In the intra-class analysis only tests involving the image 5.F lead to a number of $p-$values slightly larger than $\alpha \times 1000 = 200$, for which H_0 is rejected[1]. In all the other cases, the test accepts the H_0 hypothesis (see left-side Table 2). Conversely in the inter-classes analysis all the obtained numbers of $p-$values are much higher than 200 (right-side table). This means that, to properly compare excursion set of a given level u for images belonging to different classes, a previous *effective level* scaling is necessary.

Finally, we provide a graphical illustration of the test in (24) for three couple of images (2.F and 3.F, first panel; 1.F versus 5.D, second panel; 1.F and 3.FG, third panel). In bold marked points we represent the cases when the test (24) rejects H_0 for at level $\alpha = 0.2$. These points are drawn on the estimates $\widehat{s}_u$, for 1000 values of u. Coherently, the test accepts H_0 (see Table 2) in the first panel of Figure 4 (intra-classes analysis) excepted for some extreme values of level u. Conversely, the test (24) rejects the H_0 hypothesis for the values of u in the consider grid in the last two panels of Figure 4 (inter-classes analysis).

[1]The same atypical behavior for figure 5.F has been previously observed in Biermé et al. (2019), where the same data-set is studied.

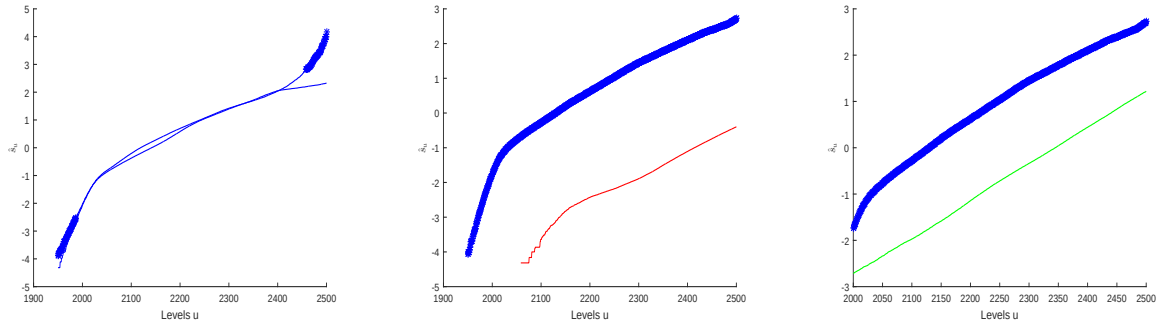

Figure 4: Synthetic digital mammograms study. Estimation of $\widehat{s}_u$ for 1000 different values of u and couples of images: 2.F and 3.F (first panel); 1.F versus 5.D (second panel); 1.F and 3.FG (third panel). In bold marked points we represent the cases where the test (24) rejects H_0 for a significant level $\alpha = 0.2$. Group (F) is displayed using blue curves, (FG) green curves and (D) red ones.

4.2 Comparing images of excursion sets: a real digital mammograms study

The data-set The Mammographic Image Analysis Society (MIAS) is an organisation of UK research groups interested in the understanding of mammograms and has produced a database of real digital mammograms. The range of intensity in all images is represented from 0 to 255 and we consider images size of 250 × 250 pixels. We study 211 mammograms classified in terms of the character of background tissue: fatty tissue group (F) (66 images), fatty-glandular (FG) (67 images), and dense (D) (77 images). Mammographic images are available online: `http://peipa.essex.ac.uk/info/mias.html` (see also Suckling et al. (1994)). One image of each group is displayed in Figure 5.

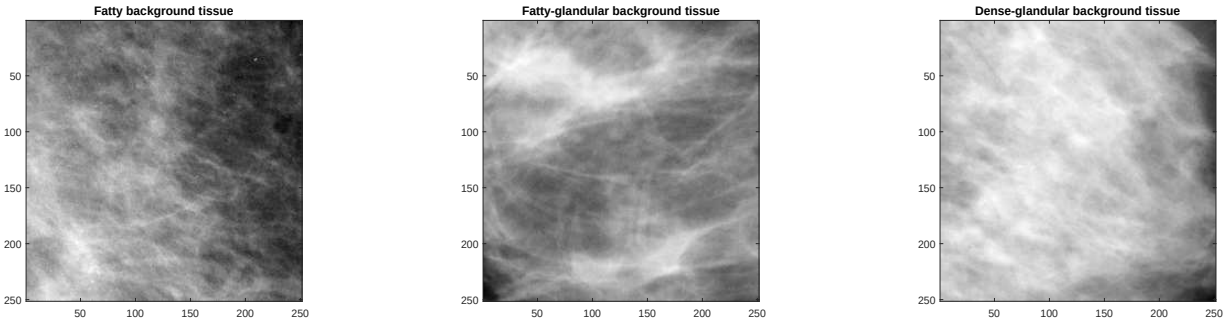

Figure 5: Real digital mammograms study. Image from group fatty background tissue (F) (left), from group fatty-glandular (FG) (center) and from group dense (D) (right). Image size: 251 × 251.

Inference and testing for *effective level* For this real mammograms data-set, similarly to Figure 4, we perform test in (24) and we display in bold marked points the cases when the test rejects H_0 for a significant level $\alpha = 0.2$ (see Figure 6 below). These points are drawn on the estimates $\widehat{s}_u$, for the considered values of u. For the sake of brevity we only display here the inter-classes analysis. Notice that in the first panel of Figure 6 we choose the difficult comparison between the two closest images between groups F and FG.

Remark that the H_0 hypothesis is accepted for almost all the level u in the considered grid in the first and the last panels of Figure 6, due to the visible proximity of the *effective levels* $\widehat{s}_u$. In the second, third and fourth panel, the H_0 hypothesis is rejected for all u and the associated excursion sets can not be

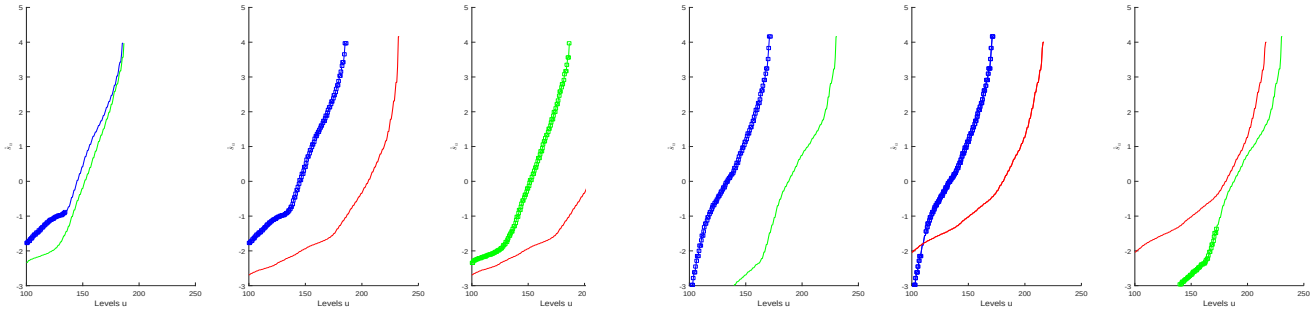

Figure 6: Real digital mammograms study. Estimation of $\widehat{s}_u$ for several levels u an a couple of images. From left to right: 1.F versus 1.FG, 1.F versus 1.D, 1.FG versus 1.D, 27.F versus 19.FG, 27.F versus 20.D, 19.FG versus 20.D. In bold marked points we represent the relative u values such that the test (24) rejects H_0 for a significant level $\alpha = 0.2$. Group (F) is displayed using blue curves, (FG) green curves and (D) red ones.

compared without a preliminary image processing. The fifth panel in Figure 6 represents an interesting hybrid situation. Almost everywhere H_0 is rejected except for a small interval of u's values where H_0 is accepted. In this small range of u, the relative excursion sets can be considered visually similar.

Analogously to Table 2 in Appendix B, we now perform the test (24) to compare all possible combinations of excursion sets of images in this data-set in a grid of 200 values of level $u \in [100, 240]$. In boxplots of Figure 7 we gathered of number of $p-$values that are smaller than the significant level $\alpha = 0.2$. The reference value is represented by the horizontal line at level $\alpha \times 200 = 40$, above which H_0 is rejected.

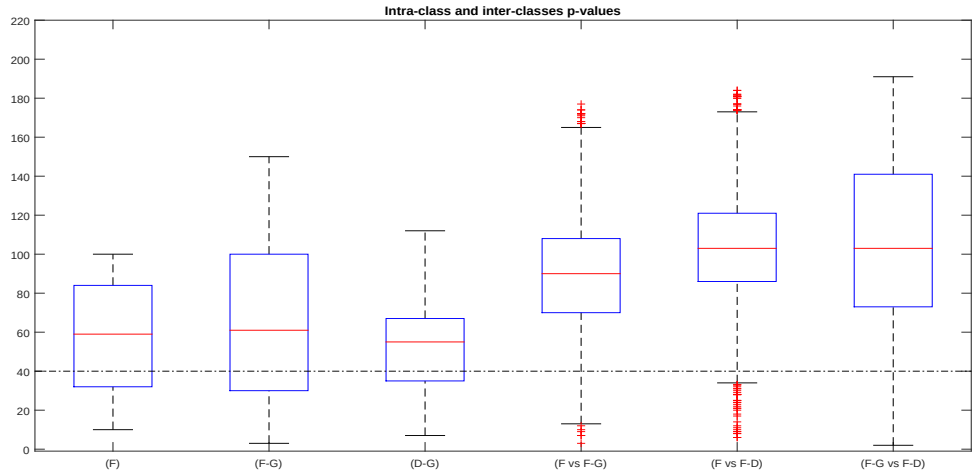

Figure 7: Real digital mammograms study. **Intra and inter-classes analysis** for the test to comparing images from the consider 3 groups. We display the boxplots of number of $p-$values associated to the 200 different values of $u \in [100, 240]$ that are smaller than the significant level $\alpha = 0.2$. In horizontal line we display the reference threshold $\alpha \times 200 = 40$, above which H_0 is rejected.

As one can expect, in Figure 7 we observe differences in terms of the medians and of the variances: the intra-classes boxplots (first three boxplots) have smaller median and variance values with respect to the inter-classes ones (last three boxplots). As in Section 4.1, this study suggests that the *effective level*

scaling procedure seems to be necessary especially in the comparison of two images of excursion sets belonging to two different background tissue groups.

5 Conclusions and discussion

In this paper, we have presented new statistics based on the average LK curvatures of the excursion set of a stationary non-standard isotropic Gaussian field X on $\mathbb{R}^2$, in particular on the Euler characteristic, the half perimeter and the area. These tools allow to built consistent inference procedures based only on a sparse observation of the Gaussian 2D random field with unknown location and scale parameters. A byproduct is the construction of a test to determine if two images of excursion sets can be compared. Here we discuss some potential improvements of the results proposed in this work.

Firstly, notice that in Sections 3.2 and 4, our testing procedure results relied mostly on the area and not on the Euler characteristic devise. The reason being that for the Euler characteristic we did not fully establish the consistency of its asymptotic variance estimator, therefore limiting the possibility to properly calibrate statistical procedures. If Conjecture 3.1 was proved, this would enlarge the options for testing and inference. Besides, if a joint auto-normalized central limit theorem for $\left(C_0^{/T}(X,u), C_2^{/T}(X,u)\right)$ was available, this would imply results on the joint behavior of $(\widehat{s}_{u,T}, \widehat{a}_{u,T})$ in Definition 2.1 and the possibility to build consolidated tests using both quantities.

Secondly, inspired by the analysis of Sections 4.1 and 4.2, the *effective level* could be useful to build a "classification criterion" between the three groups (F), (FG) and (D). Indeed, the estimated $\widehat{s}_u$ seems globally able to distinguish images coming from different groups relying exclusively on the sparse information of the excursion set with a same level u.
To explore this idea, in Figure 8 we represent for the real digital data-set the adaptive level u (y axis) for all considered 211 images such that the estimated *effective level* $\widehat{s}_u$ is approximated equal to δ, for several values of δ and where the different groups are distinguished in notation.

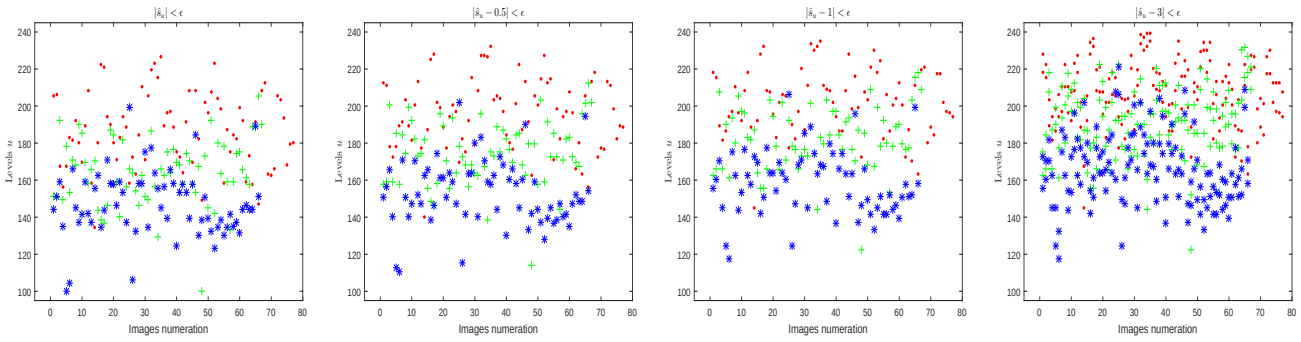

Figure 8: Real digital mammograms study. Adaptive level u (*i.e.*, level u such that s_u is close to a given value δ, y axis) for all images (x axis), such that $|\widehat{s}_u - \delta| < \epsilon$, for $\epsilon = 10^{-2}$ and $\delta = 0$ (first panel) $\delta = 0.5$ (second panel), $\delta = 1$ (third panel) and $\delta = 3$ (fourth panel). Images from group fatty (F) are displayed by blue starts, fatty-glandular group (FG) by green crosses and dense group (D) by red points.

Visually, it appears that for small values of δ (*i.e.*, for intermediate values of u) the groups might be classified from their *effective level*. Obviously, for large values of δ (*i.e.*, for extreme values of u) the quality of the separation of groups is less good, as one can expect (see last panel of Figure 8). Moreover, one can expect that for large values of the level u, the obtained classes will be more distant also due to the large variance of the *effective level* estimator (see Corollary 2.1). However globally, this tool seems

adequate to recognize the underlying background breast tissue. However an investigation on a rigorous classification procedure based on *effective levels* remains an open point and is left for future works.

Finally, in the present paper, the empirical estimator of the variance is obtained from the cutting of the domain $T^{(N)}$, as described in Section 3.1 and illustrated in Figure 1. While the theoretical constraints of the cutting procedure are clear, its practical and numerical implementation has to be treated carefully. Indeed we need simultaneously that $M_N \to \infty$ (*i.e.*, a large number of subwindow domains) and that $\mathrm{dist}(V^{(N,(i,j))}, V^{(N,(i',j'))}) \to \infty$ (*i.e.*, the size of each subwindow domain is large). As previously described in Bulinski et al. (2012), this is the crucial and well known compromise between variance and bias. Indeed, Bulinski et al. (2012) provide a numerical study in the very specific case of a spherical covariance model to find the best subwindow size in order to minimize the mean error for the variance estimator for three intermediate levels u. The appropriate size and the form (*e.g.*, square, rectangular, ...) of the subwindow is a crucial issue in applications (see Section 4). Furthermore, the cutting of $T^{(N)}$ has to guarantee that in each subwindow one can find observations of the excursion set at the chosen level $u \in \mathbb{R}$. Then, the subwindow procedure is also implicitly related to the choice of the (intermediate, large or extremes) value of observation level u.

Acknowledgments: The authors are grateful to Anne Estrade for fruitful discussions. The authors acknowledge Z. Li, (GE Healthcare France, department *Mammography*) for simulated 2D digital mammograms data-sets in Section 4.1 and the related discussion. Mammographic Image Analysis Society database can be found here `http://peipa.essex.ac.uk/info/mias.html`. This work has been partially supported by the project ANR MISTIC (ANR-19-CE40-0005).

References

Adler, R. J., Subag, E., and Taylor, J. E. (2012). Rotation and scale space random fields and the Gaussian kinematic formula. *The Annals of Statistics*, 40(6):2910–2942.

Adler, R. J. and Taylor, J. E. (2007). *Random fields and geometry*. Springer Monographs in Mathematics. Springer, New York.

Adler, R. J. and Taylor, J. E. (2011). *Topological complexity of smooth random functions*, volume 2019 of *Lecture Notes in Mathematics*. Springer, Heidelberg. Lectures from the 39th Probability Summer School held in Saint-Flour, 2009, École d'Été de Probabilités de Saint-Flour. [Saint-Flour Probability Summer School].

Azaïs, J. M. and Wschebor, M. (2009). *Level sets and extrema of random processes and fields*. John Wiley & Sons.

Berzin, C. (2018). Estimation of Local Anisotropy Based on Level Sets. *ArXiv e-prints:1801.03760*.

Biermé, H. and Desolneux, A. (2016). On the perimeter of excursion sets of shot noise random fields. *The Annals of Probability*, 44(1):521–543.

Biermé, H., Di Bernardino, E., Duval, C., and Estrade, A. (2019). Lipschitz-Killing curvatures of excursion sets for two-dimensional random fields. *Electronic Journal of Statistics*, 13(1):536–581.

Breuer, P. and Major, P. (1983). Central limit theorems for non-linear functionals of Gaussian fields. *Journal of Multivariate Analysis*, 13(3):425–441.

Bulinski, A., Spodarev, E., and Timmermann, F. (2012). Central limit theorems for the excursion set volumes of weakly dependent random fields. *Bernoulli*, 18(1):100–118.

Casaponsa, B., Crill, B., Colombo, L., Danese, L., Bock, J., Catalano, A., Bonaldi, A., Basak, S., Bonavera, L., Coulais, A., et al. (2016). Planck 2015 results: Xvi. Isotropy and statistics of the CMB.

David, O. S. and Worsley, K. (1995). Testing for a Signal with Unknown Location and Scale in a Stationary Gaussian Random Field. *The Annals of Statistics*, 23(2):608–639.

Di Bernardino, E., Estrade, A., and León, J. R. (2017). A test of Gaussianity based on the Euler characteristic of excursion sets. *Electronic Journal of Statistics*, 11(1):843–890.

Ebner, B., Henze, N., Klatt, M. A., and Mecke, K. (2018). Goodness-of-fit tests for complete spatial randomness based on Minkowski functionals of binary images. *Electronic Journal of Statistics*, 12(2):2873–2904.

Epps, T. (1987). Testing that a stationary time series is Gaussian. *The Annals of Statistics*, pages 1683–1698.

Estrade, A. and León, J. (2016). A Central Limit Theorem for the Euler characteristic of a Gaussian excursion set. *Annals of Probability*, 44(6):3849–3878.

Gott, J. R., Colley, W. N., Park, C.-G., Park, C., and Mugnolo, C. (2007). Genus topology of the cosmic microwave background from the WMAP 3-year data. *Monthly Notices of the Royal Astronomical Society*, 377(4):1668–1678.

Gott, J. R., Hambrick, D. C., Vogeley, M. S., Kim, J., Park, C., Choi, Y.-Y., Cen, R., Ostriker, J. P., and Nagamine, K. (2008). Genus topology of structure in the sloan digital sky survey: Model testing. *The Astrophysical Journal*, 675(1):16.

Hug, D., Last, G., and Schulte, M. (2016). Second-order properties and central limit theorems for geometric functionals of Boolean models. *The Annals of Applied Probability*, 26(1):73–135.

Kratz, M. and Vadlamani, S. (2018). Central limit theorem for Lipschitz–Killing curvatures of excursion sets of Gaussian random fields. *Journal of Theoretical Probability*, 31(3):1729–1758.

Lachièze-Rey, R. (2017). Shot-noise excursions and non-stabilizing Poisson functionals. *to appear in Annals of Applied Probability*.

Li, Z., Desolneux, A., Muller, S., and Carton, A. K. (2016). A novel 3D stochastic solid breast texture model for X-Ray breast imaging. In Tingberg, A., Lång, K., and Timberg, P., editors, *Breast Imaging*, pages 660–667, Cham. Springer International Publishing.

Lindgren, G. (2000). Wave analysis by Slepian models. *Probabilistic engineering mechanics*, 15(1):49–57.

Longuet-Higgins, M. S. (1957). The statistical analysis of a random, moving surface. *Philosophical Transactions of the Royal Society A*, 249(966):321–387.

Marinucci, D. and Rossi, M. (2015). Stein-Malliavin approximations for nonlinear functionals of random eigenfunctions on S^d. *Journal of Functional Analysis*, 268(8):2379 – 2420.

Mattfeldt, T., Meschenmoser, D., Pantle, U., and Schmidt, V. (2011). Characterization of mammary gland tissue using joint estimators of Minkowski functionals. *Image Analysis & Stereology*, 26(1):13–22.

Müller, D. (2017). A central limit theorem for Lipschitz–Killing curvatures of Gaussian excursions. *Journal of Mathematical Analysis and Applications*, 452(2):1040–1081.

Nieto-Reyes, A., Cuesta-Albertos, J. A., and Gamboa, F. (2014). A random-projection based test of Gaussianity for stationary processes. *Computational Statistics & Data Analysis*, 75:124–141.

Nourdin, I. and Peccati, G. (2012). Normal approximation with Malliavin calculus. *Cambridge Tracts in Mathematics*, 192.

Pantle, U., Schmidt, V., and Spodarev, E. (2010). On the estimation of integrated covariance functions of stationary random fields. *Scandinavian Journal of Statistics*, 37(1):47–66.

Pham, V.-H. (2013). On the rate of convergence for central limit theorems of sojourn times of Gaussian fields. *Stochastic Processes and their Applications*, 123(6):2158 – 2174.

Schmalzing, J. and Górski, K. M. (1998). Minkowski functionals used in the morphological analysis of cosmic microwave background anisotropy maps. *Monthly Notices of the Royal Astronomical Society*, 297(2):355–365.

Shashkin, A. P. (2002). Quasi-associatedness of a Gaussian system of random vectors. *Russian Mathematical Surveys*, 57(6):1243–1244.

Suckling, J., Parker, J., and Dance, D. (1994). The Mammographic Image Analysis Society Digital Mammogram Database. *Exerpta Medica, International Congress Series 1069*.

Szegő, G. (1959). *Orthogonal Polynomials*. Number vol. 23,ptie. 1 in American Mathematical Society. American Mathematical Society.

Taqqu, M. S. (1977). Law of the iterated logarithm for sums of non-linear functions of Gaussian variables that exhibit a long range dependence. *Probability Theory and Related Fields*, 40(3):203–238.

Wschebor, M. (2006). *Surfaces aléatoires: mesure géométrique des ensembles de niveau*, volume 1147. Springer.

A Proofs

A.1 Preliminary results

In the following we prove two auxiliary consistency results for $\widehat{C}_{0,T^{(N)}}(X,u)$ and $\widehat{C}_{2,T^{(N)}}(X,u)$.

Proposition A.1. *Let X be a Gaussian random field satisfying Assumptions (A0) and (A2).*
(i) *Let $T_1, \ldots, T_m$ be m cubes in $\mathbb{R}^d$ such that $|T_1| = \ldots = |T_m|$ and $dist(T_i, T_j) > 0$ for all $i \neq j \in \{1,\ldots,m\}^2$. Let $u_1,\ldots,u_m$ be m levels in $\mathbb{R}$, for any integer $N>0$ and $\widehat{C}_{0,T_i^{(N)}}(X,u_i)$ as in (10), let*

$$Q_i^{(N)} := \sqrt{|T_i^{(N)}|}\,(\widehat{C}_{0,T_i^{(N)}}(X,u_i) - C_0^*(X,u_i)), \quad \text{for } \ i \in \{1,\ldots,m\}.$$

As $N \to +\infty$, $\left(Q_i^{(N)},\ldots,Q_m^{(N)}\right)$ converges in distribution to a centered Gaussian vector with covariance matrix $\mathrm{diag}(\sigma^2_{C_0^*,u_1},\ldots,\sigma^2_{C_0^*,u_m})$ where $\sigma^2_{C_0^*,u_i} < +\infty$, $\forall i \in \{1,\ldots,m\}$.

(ii) *Let T be a cube in $\mathbb{R}^d$, $u_1,\ldots,u_m$ be m levels in $\mathbb{R}$. For any integer $N>0$ and $\widehat{C}_{0,T^{(N)}}(X,u_i)$ as in (10), let*

$$S_i^{(N)} := \sqrt{|T^{(N)}|}\,(\widehat{C}_{0,T^{(N)}}(X,u_i) - C_0^*(X,u_i)), \quad \text{for } \ i \in \{1,\ldots,m\}.$$

As $N \to +\infty$, $\left(S_1^{(N)},\ldots,S_m^{(N)}\right)$ converges in distribution to a centered Gaussian vector with covariance matrix $\left(\Sigma^2_{C_0^*,(u_i,u_j)}\right)_{1\le i,j\le m}$ with $\Sigma^2_{C_0^*,(u_i,u_j)} < +\infty$, for $i,j \in \{1,\ldots,m\}$.

Proof. Let $i \in \{1,\ldots,m\}$. The ith coordinate of the considered multivariate central limit theorem can be written using the following decomposition

$$\begin{aligned}
Q_i^{(N)} &= \sqrt{|T_i^{(N)}|}(\widehat{C}_{0,T_i^{(N)}}(X,u_i) - C_0^*(X,u_i)) = \sqrt{|T_i^{(N)}|}\Big(C_0^{/T_i^{(N)}}(X,u_i) - \mathbb{E}[C_0^{/T_i^{(N)}}(X,u_i)]\Big) \\
&- \frac{1}{\pi}\sqrt{|T|}\Big(C_1^{/T_i^{(N)}}(X,u_i) - \mathbb{E}[C_1^{/T_i^{(N)}}(X,u_i)]\Big)\frac{|\partial T_i^{(N)}|_1}{|T_i^{(N)}|} \\
&+ \sqrt{|T_i^{(N)}|}\Big(C_2^{/T_i^{(N)}}(X,u_i) - \mathbb{E}[C_2^{/T_i^{(N)}}(X,u_i)]\Big)\left(\frac{1}{2\pi}\frac{|\partial T_i^{(N)}|_1^2}{|T_i^{(N)}|^2} - \frac{1}{|T_i^{(N)}|}\right) \\
&:= I_0(T_i^{(N)}) + I_1(T_i^{(N)}) + I_2(T_i^{(N)}).
\end{aligned}$$

For a Gaussian random field satisfying Assumptions (A0) and (A2), Theorem 1.1 in Kratz and Vadlamani (2018) and Theorem 2.1 in Müller (2017) give $\sqrt{|T_i^{(N)}|}\big(C_1^{/T_i^{(N)}}(X,u_i) - \mathbb{E}[C_1^{/T_i^{(N)}}(X,u_i)]\big)$ admits a Gaussian centered limit distribution and therefore $I_1(T_i^{(N)}) \xrightarrow[T\nearrow\mathbb{R}^2]{\mathbb{P}} 0$. The same discussion holds for $I_2(T_i^{(N)})$. Let

$$Z_i^{(N)} = \sqrt{|T_i^{(N)}|}(C_0^{/T_i^{(N)}}(X,u_i) - \mathbb{E}[C_0^{/T_i^{(N)}}(X,u_i)]) \ \text{ for } \ i \in \{1,\ldots,m\}.$$

One can adapt the proof of the CLT in Proposition 5 (a) in Di Bernardino et al. (2017) to prove that for X satisfying Assumptions (A0) and (A2), $X(0) \sim \mathcal{N}(\mu,\sigma^2)$ and as $N \to +\infty$, $(Z_1^{(N)},\ldots,Z_m^{(N)})$ converges in distribution to a centered Gaussian vector with diagonal covariance matrix and finite elements. Finally, applying the multivariate Slutsky's theorem we get the item **(i)**. The proof of **(ii)** comes down in a similar way using item (b) of Theorem 2.5 in Estrade and León (2016). □

Proposition A.2 (Asymptotic normality of $(\widehat{C}_{2,T^{(N)}}(X,u_1),\dots,\widehat{C}_{2,T^{(N)}}(X,u_m))$). *Let X be a Gaussian random field satisfying Assumptions (A0) and (A1). For a positive integer N, consider $T^{(N)}=\{Nt : t\in T\}$ and $\widehat{C}_{2,T^{(N)}}(X,u)$ the estimator defined in (8) built on the observation $T^{(N)}\cap E_X(u_i)$, where $u_1,\dots,u_m$ are fixed. Then,*

$$\sqrt{|T^{(N)}|}(\widehat{C}_{2,T^{(N)}}(X,u_1)-C_2^*(X,u_1),\dots,\widehat{C}_{2,T^{(N)}}(X,u_m)-C_2^*(X,u_m))$$

converges in distribution to a centered Gaussian vector with $m\times m$ covariance matrix $(\Sigma^2_{C_2^*,(u_i,u_j)})_{1\le i,j\le m}$ given by $\Sigma^2_{C_2^*,(u_i,u_j)}=\frac{1}{2\pi}\int_{\mathbb{R}^2}\int_0^{\rho(t)} g_{(u_i,u_j)}(r)\mathrm{d}r\,\mathrm{d}t\in(0,+\infty)$ where

$$g_{(u_i,u_j)}(r)=\frac{1}{\sqrt{1-r^2}}\exp\left\{-\frac{(u_i-\mu)^2-2r(u_i-\mu)(u_j-\mu)+(u_j-\mu)^2}{2\sigma^2(1-r^2)}\right\}.$$

The proof of Proposition A.2 comes down from Theorem 4 in Bulinski et al. (2012), together with Shashkin (2002) ensuring Gaussian fields are quasi-associated.

A.2 Proofs of the obtained results

Proof of Proposition 1.1

The Gaussian kinematic formula provides the mean LK curvatures of excursion sets of X within a rectangle T (see, *e.g.*, Theorem 15.9.5 in Adler and Taylor (2007) or Theorem 4.8.1, 4.3.1 in Adler and Taylor (2011)), for $u\in\mathbb{R}$ and $i=0,1,2$,

$$\mathbb{E}\left[\mathcal{L}_i(X,T,u)\right]=\sum_{l=0}^{2-i}\begin{bmatrix} i+l \\ l\end{bmatrix}(2\pi)^{-l/2}\left(\frac{\lambda}{\sigma^2}\right)^{l/2}\mathcal{M}_l(X,u)\,\mathcal{L}_{i+l}(T)$$

where $\mathcal{L}_j(T)$, $j=0,1,2$ are defined in (5), $\begin{bmatrix} i+l \\ l\end{bmatrix}=\binom{i+l}{l}\frac{\omega_{l+i}}{\omega_l\omega_i}$ with ω_k the Lebesgue measure of the k-dimensional unit ball ($w_0=1$, $w_1=2$ and $w_2=\pi$), and, following Formula (3.5.2) in Adler and Taylor (2011), the coefficients $\mathcal{M}_l(X,u)$, $l=0,1,2$ are obtained having an expansion in θ at order 2 of

$$\begin{aligned}\mathbb{P}\Big(G(0)\ge\frac{u-\mu}{\sigma}-\theta\Big) &= \psi\left(\frac{u-\mu}{\sigma}\right)-\theta\psi'\left(\frac{u-\mu}{\sigma}\right)+\frac{1}{2}\theta^2\psi''\left(\frac{u-\mu}{\sigma}\right)+O(\theta^3)\\ &= \mathcal{M}_0(X,u)+\theta\mathcal{M}_1(X,u)+\frac{1}{2}\theta^2\mathcal{M}_2(X,u)+O(\theta^3),\end{aligned}$$

where $G(0)$ is a Gaussian random variable with zero mean and unit variance and ψ its tail distribution. This concludes the proof. □

Proof of Proposition 2.2

Set $h:s\mapsto s\exp\{-s^2/2\})/(2\pi)^{3/2}$ and note that $|T_1^{(N)}|=|T_2^{(N)}|$. The ith coordinate $|T_1^{(N)}|^{1/2}(\widehat{a}_{u_i,T^{(N)}}-a)$ can be decomposed as follows

$$\sqrt{|T_1^{(N)}|}\left[\frac{h(s_{u_i})}{h(\widehat{s}_{u,2})}\left(\frac{\widehat{C}_{0,T_1^{(N)}}(X,u_i)}{h(s_{u_i})}-\frac{C_0^*(X,u_i)}{h(s_{u_i})}\right)+C_0^*(X,u_i)\left(\frac{1}{h(\widehat{s}_{u,2})}-\frac{1}{h(s_{u_i})}\right)\right],$$

where $\widehat{s}_{u,2} := \widehat{s}_{u,T_2^{(N)}}$. Since h is continuous, using Proposition 2.1 we get $h(s_{u_i})/h(\widehat{s}_{u_i,T_2^{(N)}}) \xrightarrow[N\to\infty]{\mathbb{P}} 1$, for all $1 \le i \le m$. Then, by using Propositions 2.1 and A.1, the multivariate delta method and that $\mathrm{dist}(T_1^{(N)}, T_2^{(N)}) \to \infty$ as $N \to \infty$, we obtain that $\sqrt{|T_1^{(N)}|}\big(\widehat{a}_{u_1,T^{(N)}} - a, \dots, \widehat{a}_{u_m,T^{(N)}} - a\big)$ converges in distribution to a centered Gaussian vector with covariance matrix given by $A\Sigma^2_{C_0^*}A^t + B\Sigma^2_{\frac{1}{h}}B^t$, where $.^t$ denotes the matrix transposition, A and B are the diagonal matrices

$$A = \mathrm{diag}\Big(\frac{1}{h(s_{u_1})}, \dots, \frac{1}{h(s_{u_m})}\Big), \quad B = \mathrm{diag}\Big(C_0^*(X,u_1), \dots, C_0^*(X,u_m)\Big),$$

$\Sigma^2_{C_0^*} = \big(\Sigma^2_{C_0^*,(u_i,u_j)}\big)_{1\le i,j\le m}$ is defined in Proposition A.1, $\Sigma^2_{\frac{1}{h}} = J_{\frac{1}{h}}\Sigma^2_s J^t_{\frac{1}{h}}$ with $\Sigma^2_s = \big(\Sigma^2_{s,(u_i,u_j)}\big)_{1\le i,j\le m}$ defined in Proposition 2.1 and $J_{\frac{1}{h}}$ the $m\times m$ Jacobian matrix

$$J_{\frac{1}{h}} = (2\pi)^{\frac{3}{2}}\mathrm{diag}\left(\frac{(s_{u_1}^2-1)}{s_{u_1}^2}\exp\left\{\frac{s_{u_1}^2}{2}\right\}, \dots, \frac{(s_{u_m}^2-1)}{s_{u_m}^2}\exp\left\{\frac{s_{u_m}^2}{2}\right\}\right).$$

After computations we get $A\Sigma^2_{C_0^*}A^t = \big(\frac{\Sigma^2_{C_0^*,(u_i,u_j)}}{h(s_{u_i})h(s_{u_j})}\big)_{1\le i,j\le m}$ and

$$B\Sigma^2_{\frac{1}{h}}B^t = \left((2\pi)^3 C_0^*(X,u_i)C_0^*(X,u_j)\frac{(s_{u_i}^2-1)(s_{u_j}^2-1)}{s_{u_i}^2 s_{u_j}^2}\exp\left\{\frac{1}{2}(s_{u_i}^2+s_{u_j}^2)\right\}\Sigma^2_{s,(u_i,u_j)}\right)_{1\le i,j\le m}.$$

Adding these expressions provide the desired formula. □

Proof of Proposition 3.2

First, write

$$\begin{aligned}\sqrt{|T_1^{(N)}|}\big(\widehat{R}_{T_1^{(N)}}(u_1,u_2) - \widehat{R}^{H_0}_{T_2^{(N)}}(u_1,u_2)\big) =& \sqrt{|T_1^{(N)}|}\big(\widehat{R}_{T_1^{(N)}}(u_1,u_2) - R^{H_0}(u_1,u_2)\big) \\ &+ \sqrt{|T_2^{(N)}|}\big(R^{H_0}(u_1,u_2) - \widehat{R}^{H_0}_{T_2^{(N)}}(u_1,u_2)\big).\end{aligned} \tag{25}$$

For the first term in (25) we use Proposition A.1 **(ii)** and the delta method with the function $g : (x,y) \mapsto \frac{x}{y}$. We get after computations, using that $\widehat{R}_{T_1}(u_1,u_2) = g\big(\widehat{C}_{0,T_1}(X,u_2), \widehat{C}_{0,T_1}(X,u_1)\big)$,

$$\sqrt{|T_1^{(N)}|}\Big(g\big(\widehat{C}_{0,T_1^{(N)}}(X,u_2), \widehat{C}_{0,T_1^{(N)}}(X,u_1)\big) - g\big(C_0^*(X,u_2), C_0^*(X,u_1)\big)\Big) \xrightarrow[N\to\infty]{d,\ H_0} \mathcal{N}\Big(0, \sigma^2_{g(C_0^*),(u_1,u_2)}\Big)$$

where

$$\sigma^2_{g(C_0^*),(u_1,u_2)} = \frac{\sigma^2_{C_0^*,u_2}}{C_0^*(X,u_1)^2} - 2\frac{C_0^*(X,u_2)}{C_0^*(X,u_1)^3}\Sigma^2_{C_0^*,(u_1,u_2)} + \frac{C_0^*(X,u_2)^2}{C_0^*(X,u_1)^4}\sigma^2_{C_0^*,u_1}.$$

For the second term in (25) we use Proposition 2.1 and apply the delta method with the function $h : (x,y) \mapsto \frac{x}{y}\exp\{-\frac{1}{2}(x^2-y^2)\}$. We get after computations, using that $\widehat{R}^{H_0}_{T_2^{(N)}}(u_1,u_2) = h(\widehat{s}_{u_2,T_2^{(N)}}, \widehat{s}_{u_1,T_2^{(N)}})$,

$$\sqrt{|T_2^{(N)}|}\Big(h(s_{u_2},s_{u_1}) - h(\widehat{s}_{u_2,T_2^{(N)}}, \widehat{s}_{u_1,T_2^{(N)}})\Big) \xrightarrow[N\to\infty]{d,\ H_0} \mathcal{N}\Big(0, \sigma^2_{h(s),(u_1,u_2)}\Big)$$

where $\sigma^2_{h(s),(u_1,u_2)} = \nabla h(s_{u_2},s_{u_1})'\Sigma^2_{s,(u_1,u_2)}\nabla h(s_{u_2},s_{u_1})$, $\Sigma^2_{s,(u_1,u_2)}$ is defined as in Proposition 2.1,

$$\sigma^2{}_{h(s),(u_1,u_2)} = \mathrm{e}^{-(s_{u_2}^2-s_{u_1}^2)}\Big[\sigma^2_{s_{u_2}}\Big(\frac{1-s_{u_2}^2}{s_{u_1}}\Big)^2 + 2\Sigma^2_{s,(u_1,u_2)}\Big(\frac{1-s_{u_2}^2}{s_{u_1}}\Big)\Big(-\frac{s_{u_2}}{s_{u_1}^2}+s_{u_2}\Big) + \sigma^2_{s_{u_1}}\Big(-\frac{s_{u_2}}{s_{u_1}^2}+s_{u_2}\Big)^2\Big].$$

Using $\mathrm{dist}(T_1^{(N)}, T_2^{(N)}) \to \infty$ as $N \to \infty$ and $\sigma^2_{R_{u_1,u_2}} = \sigma^2_{g(C_0^*),(u_1,u_2)} + \sigma^2_{h(s),(u_1,u_2)}$ we get the result. □

Proof of Proposition 3.3

Since J is a finite set and using Corollary 3.1, it immediately holds that

$$\left(\widehat{\sigma}^2_{s_{u_1}}, \dots, \widehat{\sigma}^2_{s_{u_J}}\right) \xrightarrow[T\nearrow\mathbb{R}^2]{\mathbb{P}} \left(\sigma^2_{s_{u_1}}, \dots, \sigma^2_{s_{u_J}}\right).$$

Denote by $j^* = \operatorname{argmin}_{j\in\{1,\dots,J\}}\sigma^2_{s_{u_j}}$, it follows

$$\begin{aligned}
\mathbb{P}(\widehat{j} \neq j^*) &= \mathbb{P}\Big(\bigcup_{j\neq j^*}\{\widehat{\sigma}^2_{s_{u_j}} \leq \widehat{\sigma}^2_{s_{u_{j^*}}}\}\Big) \leq \sum_{j\neq j^*}\mathbb{P}(\widehat{\sigma}^2_{s_{u_j}} - \sigma^2_{s_{u_j}} + (\sigma^2_{s_{u_j}} - \sigma^2_{s_{u_{j^*}}}) \leq \widehat{\sigma}^2_{s_{u_{j^*}}} - \sigma^2_{s_{u_{j^*}}}) \\
&\leq \sum_{j\neq j^*}\mathbb{P}(|\sigma^2_{s_{u_j}} - \sigma^2_{s_{u_{j^*}}}| \leq |\widehat{\sigma}^2_{s_{u_{j^*}}} - \sigma^2_{s_{u_{j^*}}}| + |\widehat{\sigma}^2_{s_{u_j}} - \sigma^2_{s_{u_j}}|) \\
&\leq \sum_{j\neq j^*}\Big(\mathbb{P}(\tfrac{1}{2}|\sigma^2_{s_{u_j}} - \sigma^2_{s_{u_{j^*}}}| \leq |\widehat{\sigma}^2_{s_{u_{j^*}}} - \sigma^2_{s_{u_{j^*}}}|) + \mathbb{P}(\tfrac{1}{2}|\sigma^2_{s_{u_j}} - \sigma^2_{s_{u_{j^*}}}| \leq |\widehat{\sigma}^2_{s_{u_j}} - \sigma^2_{s_{u_j}}|)\Big) \xrightarrow[T\nearrow\mathbb{R}^2]{} 0,
\end{aligned}$$

where we used that J is finite, $\forall j \neq j^*$, $|\sigma^2_{s_{u_j}} - \sigma^2_{s_{u_{j^*}}}| > 0$ and Corollary 3.1. Finally, we derive that $\widehat{j} \xrightarrow{\mathbb{P}} j^*$, for $T \nearrow \mathbb{R}^2$, together with the definition of j^* and the fact that $u \mapsto \sigma^2_{s_u}$ is decreasing on $(-\infty, \mu)$ and increasing on (μ, ∞), the result follows. □

A.3 Proof of Proposition 3.1

Preliminaries on the Itô-Wiener chaos decomposition for $\mathcal{L}_2$ Let $G := (X-\mu)/\sigma$ be the centered and unit variance Gaussian random field associated to X, for all fixed level u. Recall that $s_u = (u-\mu)/\sigma$, then $\mathcal{L}_{2,T}(X,u) = \mathcal{L}_{2,T}(G, s_u)$, which is a square-integrable functional of the Gaussian field G. It admits an orthogonal decomposition into Itô-Wiener chaos in the L^2 sense (see, *e.g.*, Marinucci and Rossi (2015), Nourdin and Peccati (2012)):

$$\mathcal{L}_2(G, s_u, T) = \sum_{q=0}^{+\infty}\frac{\beta_q(s_u)}{q!}\int_T H_q(G(t))\,\mathrm{d}t,$$

where H_q is the q-th Hermite polynomial, *i.e.*, for $z \in \mathbb{R}$, $H_0(z) = 1$ and

$$H_q(z) = (-1)^q \exp\{z^2/2\}\frac{\mathrm{d}^q}{\mathrm{d}z^q}\exp\{-z^2/2\}, \quad \text{if } q \geq 1.$$

The above series converges in $L^2(\mathbb{P})$ and for $Z \sim \mathcal{N}(0,1)$, $\beta_q(s_u) := \mathbb{E}\left[\mathbf{1}_{\{Z\geq s_u\}}H_q(Z)\right]$. The chaotic coefficients $(\beta_q(s_u))_{q\geq 0}$ for $\mathcal{L}_2(G, s_u, T)$ are given by: $\beta_0(s_u) = \psi(s_u)$ and

$$\beta_q(s_u) = \int_{s_u}^{+\infty}\varphi(z)\frac{(-1)^q}{\varphi(z)}\frac{\mathrm{d}^q}{\mathrm{d}z^q}\varphi(z)\mathrm{d}z = (-1)^{q-1}\frac{\mathrm{d}^{q-1}}{\mathrm{d}z^{q-1}}\varphi(s_u) = \varphi(s_u)H_{q-1}(s_u),$$

for $q \geq 1$, where φ is the probability density function of Z. Denoting H_q^ϕ the "physicist Hermite polynomials" we have $H_q^\phi(x) = 2^{q/2}H_q(\sqrt{2}x)$ and it holds $\forall x$, $|(2^q q!\sqrt{\pi})^{-1/2}H_q^\phi(x)e^{-x^2/2}| \leq C_\infty/(q+1)^{1/12}$ (see Szegő (1959) for the the value of the constant C_∞). As, it holds $\forall x \in \mathbb{R}$

$$H_q^\phi(x)e^{-x^2/2} = 2^{q/2}H_q(\sqrt{2}x)e^{-x^2/2} = e^{x^2/2}2^{q/2}H_q(\sqrt{2}x)e^{-(\sqrt{2}x)^2/2},$$

it follows $\forall x \in \mathbb{R}$

$$|\beta_{q+1}(\sqrt{2}x)| = |H_q(\sqrt{2}x)e^{-(\sqrt{2}x)^2/2}| \leq e^{-x^2/2}\sqrt{q!\sqrt{\pi}}C_\infty/(q+1)^{\frac{1}{12}} \leq C_\infty \pi^{\frac{1}{4}} \frac{\sqrt{q!}}{(q+1)^{\frac{1}{12}}}.$$

We derive the following inequality, frequently used in the sequel

$$\|\beta_0\|_\infty \leq 1 \quad \text{and} \quad \|\beta_q\|_\infty \leq c_\beta \frac{\sqrt{(q-1)!}}{q^{\frac{1}{12}}}, \quad q \geq 1. \tag{26}$$

The mean of $\mathcal{L}_2(G, s_u, T)$ is its projection onto the 0-th Itô-Wiener chaos $\mathbb{E}\left[\mathcal{L}_2(G, s_u, T)\right] = \psi(s_u)|T|$. The remaining of the proof consist in controlling the order of the fourth moment of $\mathcal{L}_2(G, s_\cdot, T)$, computed using the chaos decomposition as follows

$$\begin{aligned}
&\mathbb{E}[\mathcal{L}_2(G, s_{u_1}, T)\mathcal{L}_2(G, s_{u_2}, T)\mathcal{L}_2(G, s_{u_3}, T')\mathcal{L}_2(G, s_{u_4}, T')] \\
&\quad = \sum_{k_1,k_2,k_3,k_4=0}^{+\infty} \frac{\beta_{k_1}(s_{u_1})\beta_{k_2}(s_{u_2})\beta_{k_3}(s_{u_3})\beta_{k_4}(s_{u_4})}{k_1!k_2!k_3!k_4!} \\
&\qquad\qquad \times \int_T \int_T \int_{T'} \int_{T'} \mathbb{E}[H_{k_1}(G(t_1))H_{k_2}(G(t_2))H_{k_3}(G(t_3))H_{k_4}(G(t_4))]\,\mathrm{d}t_1\,\mathrm{d}t_2\,\mathrm{d}t_3\,\mathrm{d}t_4.
\end{aligned}$$

Control of a fourth moment of $\mathcal{L}_2(G, s_\cdot, T)$ We sometimes denote $T_1 = T_2 := T$ and $T_3 = T_4 := T'$ and use that $|T| = |T'|$. We write,

$$\mathbb{E}[\mathcal{L}_2(G, s_{u_1}, T)\mathcal{L}_2(G, s_{u_2}, T)\mathcal{L}_2(G, s_{u_3}, T')\mathcal{L}_2(G, s_{u_4}, T')] = V_0 + V_1 + V_2 + V_3 + V_4, \tag{27}$$

where

$$\begin{aligned}
V_0 &:= |T|^4 \beta_0(s_{u_1})\beta_0(s_{u_2})\beta_0(s_{u_3})\beta_0(s_{u_4}) \\
V_1 &:= |T|^3 \sum_{j=1}^4 \frac{\beta_0(s_{u_1})\beta_0(s_{u_2})\beta_0(s_{u_3})\beta_0(s_{u_4})}{\beta_0(s_{u_j})} \sum_{k_j=1}^{+\infty} \frac{\beta_{k_j}(s_{u_j})}{k_j!} \int_{T_j} \mathbb{E}[H_{k_j}(G(t_j))]\,\mathrm{d}t_j
\end{aligned}$$

$$V_2 := |T|^2 \sum_{j_1 \neq j_2 \in \{1,\dots,4\}} \sum_{\substack{k_{i_1}, k_{i_2} = 1 \\ i_1, i_2 \neq j_1, j_2}}^{+\infty} \frac{\beta_{k_{i_1}}(s_{u_{i_1}})\beta_{k_{i_2}}(s_{u_{i_2}})\beta_0(s_{u_{j_1}})\beta_0(s_{u_{j_2}})}{k_{i_1}!k_{i_2}!} \int_{T_{i_1}} \int_{T_{i_2}} \mathbb{E}[H_{k_{i_1}}(G(t_{i_1}))H_{k_{i_2}}(G(t_{i_2}))]\,\mathrm{d}t_{i_1}\,\mathrm{d}t_{i_2}$$

$$\begin{aligned}
V_3 &:= |T| \sum_{j=1}^4 \beta_0(s_{u_j}) \sum_{\substack{k_{i_1}, k_{i_2}, k_{i_3} = 1 \\ i_1 \neq j, i_2 \neq j, i_3 \neq j}}^{+\infty} \frac{\beta_{k_{i_1}}(s_{u_{i_1}})\beta_{k_{i_2}}(s_{u_{i_2}})\beta_{k_{i_3}}(s_{u_{i_3}})}{k_{i_1}!k_{i_2}!k_{i_3}!} \\
&\qquad \times \int_{T_{i_1}} \int_{T_{i_2}} \int_{T_{i_3}} \mathbb{E}[H_{k_{i_1}}(G(t_{i_1}))H_{k_{i_2}}(G(t_{i_2}))H_{k_{i_3}}(G(t_{i_3}))]\,\mathrm{d}t_{i_1}\,\mathrm{d}t_{i_2}\,\mathrm{d}t_{i_3}
\end{aligned}$$

$$\begin{aligned}
V_4 &:= \sum_{k_1,k_2,k_3,k_4=1}^{+\infty} \frac{\beta_{k_1}(s_{u_1})\beta_{k_2}(s_{u_2})\beta_{k_3}(s_{u_3})\beta_{k_4}(s_{u_4})}{k_1!k_2!k_3!k_4!} \\
&\qquad \times \int_T \int_T \int_{T'} \int_{T'} \mathbb{E}[H_{k_1}(G(t_1))H_{k_2}(G(t_2))H_{k_3}(G(t_3))H_{k_4}(G(t_4))]\,\mathrm{d}t_1\,\mathrm{d}t_2\,\mathrm{d}t_3\,\mathrm{d}t_4.
\end{aligned}$$

It holds $V_0 = \psi(s_{u_1})\psi(s_{u_2})\psi(s_{u_3})\psi(s_{u_4})|T|^4$ and by orthogonality of H_{k_1} with $H_0 = 1$, $\forall\, k_1 \geq 1$, we get $V_1 = 0$. It remains to control the terms V_2, V_3 and V_4.

Control of V_2. Using the fact that $\mathbb{E}[H_k(G(t))H_l(G(s))] = \delta_{k,l}k!\rho(t-s)^k$ (see *e.g.* Equation (2.1) in Breuer and Major (1983)), we get

$$\begin{aligned}
V_2 &= |T|^2 \sum_{j_1 \neq j_2 \in \{1,\dots,4\}} \beta_0(s_{u_{j_1}})\beta_0(s_{u_{j_2}}) \sum_{\substack{k=1 \\ i_1,i_2 \neq j_1,j_2}}^{+\infty} \frac{\beta_k(s_{u_{i_1}})\beta_k(s_{u_{i_2}})}{k!} \int_{T_{i_1}}\int_{T_{i_2}} \rho(t_{i_1}-t_{i_2})^k \,\mathrm{d}t_{i_1}\,\mathrm{d}t_{i_2} \\
&= |T|^2 \Big(\sum_{j_1 \neq j_2 \in \mathcal{I}_{2,1}} + \sum_{j_1 \neq j_2 \in \mathcal{I}_{2,2}} \Big) \beta_0(s_{u_{j_1}})\beta_0(s_{u_{j_2}}) \sum_{\substack{k=1 \\ i_1,i_2 \neq j_1,j_2}}^{+\infty} \frac{\beta_k(s_{u_{i_1}})\beta_k(s_{u_{i_2}})}{k!} \int_{T_{i_1}}\int_{T_{i_2}} \rho(t_{i_1}-t_{i_2})^k \,\mathrm{d}t_{i_1}\,\mathrm{d}t_{i_2} \\
&=: V_{2,1} + V_{2,2},
\end{aligned}$$

where $\mathcal{I}_{2,1} := \{(1,3),(1,4),(2,3),(2,4)\}$ and $\mathcal{I}_{2,2} := \{(1,2),(3,4)\}$. Using (26) and that the correlation function ρ is decreasing together with the fact that on $\mathcal{I}_{2,1}$ the integration is made on distinct rectangles T and T', we get

$$\begin{aligned}
|V_{2,1}| &\leq 4c_\beta^2|T|^2 \sum_{k=1}^{+\infty} \frac{(k-1)!}{k!k^{1/6}} \int_T\int_{T'} |\rho(t-t')|^k \,\mathrm{d}t\,\mathrm{d}t' \leq 4c_\beta^2|T|^2 \sum_{k=1}^{+\infty} \frac{1}{k^{1+1/6}} \int_T\int_{T'} \frac{1}{(1+\|t-t'\|)^{\gamma k}} \,\mathrm{d}t\,\mathrm{d}t' \\
&\leq 4c_\beta^2|T|^2 \sum_{k=1}^{+\infty} \frac{1}{k^{1+1/6}} \frac{1}{\mathrm{dist}(T,T')^{\gamma k-2}} \int_T\int_{T'} \frac{1}{(1+\|t-t'\|)^2} \,\mathrm{d}t\,\mathrm{d}t' \\
&\leq 4c_\beta^2|T|^2 \sum_{k=1}^{+\infty} \frac{1}{\mathrm{dist}(T,T')^{\gamma k-2}} \int_{\mathbb{R}^2} \frac{1}{(1+\|t-t'\|)^2} \,\mathrm{d}t\,\mathrm{d}t' \leq C_{2,1} \frac{|T|^2}{\mathrm{dist}(T,T')^{\gamma-2}},
\end{aligned}$$

where we used Assumption ($\mathcal{A}1$) and $\mathrm{dist}(T,T') > 2$, then $C_{2,1}$ is given by $8c_\beta^2 \int_{\mathbb{R}^2}(1+\|t-t'\|)^{-2}\mathrm{d}t\,\mathrm{d}t'$. For $V_{2,2}$, using (26) and Assumption ($\mathcal{A}1$), we have

$$\begin{aligned}
|V_{2,2}| &\leq |T|^2 \Big(|\beta_0(s_{u_1})\beta_0(s_{u_2})| \sum_{k=1}^{\infty} \frac{|\beta_k(s_{u_3})\beta_k(s_{u_4})|}{k!} \int_{T'}\int_{T'} |\rho(t-s)|^k \mathrm{d}t\,\mathrm{d}s \\
&\qquad + |\beta_0(s_{u_3})\beta_0(s_{u_4})| \sum_{k=1}^{\infty} \frac{|\beta_k(s_{u_1})\beta_k(s_{u_2})|}{k!} \int_T\int_T |\rho(t-s)|^k \mathrm{d}t\,\mathrm{d}s \Big) \\
&\leq 2c_\beta^2|T|^2 \sum_{k=1}^{\infty} \frac{1}{k^{1+1/6}} \int_T\int_T \frac{\mathrm{d}t\,\mathrm{d}s}{(1+\|t-s\|)^\gamma} \leq C_{2,2}|T|^2,
\end{aligned}$$

where $C_{2,2} = 2c_\beta^2 \int_{\mathbb{R}^2}(1+\|t-t'\|)^{-2}\mathrm{d}t\,\mathrm{d}t' \sum_{k\geq 1} k^{-1-\frac{1}{6}}$ is a constant independent of T. It follows that $V_2 = O(|T|^2)$.

Control of V_3. To control this term we rely on the diagram formula and the following decomposition

$$\begin{aligned}
V_3 &= |T| \sum_{j=1}^{4} \beta_0(s_{u_j}) \sum_{\substack{k_{i_1},k_{i_2},k_{i_3}=1 \\ i_1\neq j, i_2\neq j, i_3\neq j}}^{+\infty} \frac{\beta_{k_{i_1}}(s_{u_{i_1}})\beta_{k_{i_2}}(s_{u_{i_2}})\beta_{k_{i_3}}(s_{u_{i_3}})}{k_{i_1}!k_{i_2}!k_{i_3}!} \\
&\qquad \times \int_{T_{i_1}}\int_{T_{i_2}}\int_{T_{i_3}} \mathbb{E}[H_{k_{i_1}}(G(t_{i_1}))H_{k_{i_2}}(G(t_{i_2}))H_{k_{i_3}}(G(t_{i_3}))]\,\mathrm{d}t_{i_1}\,\mathrm{d}t_{i_2}\,\mathrm{d}t_{i_3} \\
&= |T| \sum_{j=1}^{4} \beta_0(s_{u_j}) \Bigg(\sum_{\substack{k_{i_1},k_{i_2},k_{i_3}=1 \\ i_1\neq j, i_2\neq j, i_3\neq j \\ k_{i_1}+k_{i_2}+k_{i_3}\leq 2N_{T,T'}}}^{+\infty} + \sum_{\substack{k_{i_1},k_{i_2},k_{i_3}=1 \\ i_1\neq j, i_2\neq j, i_3\neq j \\ k_{i_1}+k_{i_2}+k_{i_3}> 2N_{T,T'}}}^{+\infty} \Bigg) \frac{\beta_{k_{i_1}}(s_{u_{i_1}})\beta_{k_{i_2}}(s_{u_{i_2}})\beta_{k_{i_3}}(s_{u_{i_3}})}{k_{i_1}!k_{i_2}!k_{i_3}!} \\
&\qquad \times \int_{T_{i_1}}\int_{T_{i_2}}\int_{T_{i_3}} \mathbb{E}[H_{k_{i_1}}(G(t_{i_1}))H_{k_{i_2}}(G(t_{i_2}))H_{k_{i_3}}(G(t_{i_3}))]\,\mathrm{d}t_{i_1}\,\mathrm{d}t_{i_2}\,\mathrm{d}t_{i_3} \\
&= V_{3,\leq N_{T,T'}} + V_{3,>N_{T,T'}},
\end{aligned}$$

for some positive integer $N_{T,T'}$ depending on T and T' and such that $N_{T,T'} \to \infty$ as $\mathrm{dist}(T,T') \to \infty$. First, note that $V_{3,>N_{T,T'}} = o(|T|^2)$ as $\mathrm{dist}(T,T') \to \infty$: using that $\mathcal{L}_2(G, s_u, T) \leq |T|$ *a.s.* and that the Itô-Wiener chaos decomposition holds in the L^2 sense, we write

$$V_{3,>N_{T,T'}} \leq C|T|^2 \max_{u\in\{u_1,u_2,u_3,u_4\}} \mathbb{E}\Big[\Big(\sum_{q\geq N_{T,T'}} \frac{\beta_q(s_u)}{q!}\int_T H_q(G(t))\mathrm{d}t\Big)^2\Big],$$

which tends to 0 as the remainder of a convergent series. To control this term, we take advantage of the cutting described in Figure 1.

We now focus on $V_{3,\leq N_{T,T'}}$, by symmetry we set $k_4 = 0$ and compute $T_{k_1,k_2,k_3} := \mathbb{E}[H_{k_1}(G_1)H_{k_2}(G_2)H_{k_3}(G_3)]$ for $k_j \geq 1$, $j \in \{1,2,3\}$ and (G_1,G_2,G_3) a standard Gaussian (see Taqqu (1977) Definition 3.1), *i.e.* a centered Gaussian vector with $\mathbb{E}[G_i^2] = 1$ and $\rho_{i,j} := \mathbb{E}[G_iG_j]$ such that $|\rho_{i,j}| \leq 1$, $1 \leq i,j \leq 3$. The diagram formula (see Taqqu (1977), Lemma 3.2) gives

$$T_{k_1,k_2,k_3} = \begin{cases} \frac{k_1!k_2!k_3!}{2^q q!} \displaystyle\sum_{\mathcal{I}(k_1,k_2,k_3)} \rho_{i_1,j_1}\dots\rho_{i_q,j_q} & \text{if } k_1+k_2+k_3 = 2q,\ 1\leq k_1,k_2,k_3 \leq q \\ 0 & \text{otherwise} \end{cases} \tag{28}$$

where the set of indices $\mathcal{I}(k_1,k_2,k_3)$ is the set of all indices $(i_1,j_1,\dots,i_q,j_q)$ such that

i) $(i_1,j_1,\dots,i_q,j_q) \in \{1,2,3\}^{2q}$,

ii) $i_1 \neq j_1,\dots,i_q \neq j_q$,

iii) there are k_1 indices 1, k_2 indices 2 and k_3 indices 3.

As $\rho_{i,j} = \rho_{j,i}$, after multiplying T_{k_1,k_2,k_3} by 2^q, $\mathcal{I}(k_1,k_2,k_3)$ simplifies in $\widetilde{\mathcal{I}}(k_1,k_2,k_3)$ the set of all indices $(i_1,j_1,\dots,i_q,j_q)$ such that

i+ii) $((i_1,j_1),\dots,(i_q,j_q)) \in \{(1,2),(1,3),(2,3)\}^q$,

iii) there are q_1 times $(1,2)$, q_2 times $(1,3)$ and q_3 times $(2,3)$ with $q_1 = k_1+k_2-q = q-k_3$, $q_2 = k_1+k_3-q = q-k_2$ and $q_3 = k_2+k_3-q = q-k_1$.

The cardinality of $\widetilde{\mathcal{I}}(k_1,k_2,k_3)$ is $\binom{q}{q_1,q_2,q_3} = \frac{q!}{q_1!q_2!q_3!}$. Set $\mathcal{J}_3(q) = \{(k_1,k_2,k_3) \in \{1,\dots,q\}^3,\ k_1+k_2+k_3 = 2q\}$, the set of indices where T_{k_1,k_2,k_3} is nonzero. Using (26), Assumption ($\mathcal{A}1$) and the cardinality of $\widetilde{\mathcal{I}}(k_1,k_2,k_3)$, it follows from (28) that,

$$
\begin{aligned}
|V_{3,\le N_{T,T'}}| \le\ & 4\,|T| \max_{u^*\in(u_1,u_2,u_3,u_4)} |\beta_0(s_{u^*})|^4 \sum_{q=4}^{N_{T,T'}} \sum_{(k_1,k_2,k_3)\in\mathcal{J}_3(q)} \frac{|\beta_{k_1}(s_{u^*})\beta_{k_2}(s_{u^*})\beta_{k_3}(s_{u^*})|}{q_1!q_2!q_3!} \\
& \times \int_T\int_T\int_{T'} |\rho(t_1-t_2)|^{q-k_3}|\rho(t_1-t_3)|^{q-k_2}|\rho(t_2-t_3)|^{q-k_1}\,\mathrm{d}t_1\,\mathrm{d}t_2\,\mathrm{d}t_3 \\
\le\ & 4c_\beta^3\,|T| \sum_{q=4}^{N_{T,T'}} \sum_{(k_1,k_2,k_3)\in\mathcal{J}_3(q)} \frac{\sqrt{(k_1-1)!(k_2-1)!(k_3-1)!}}{(k_1k_2k_3)^{\frac{1}{12}}(q-k_3)!(q-k_2)!(q-k_1)!} \\
& \times \int_T\int_T\int_{T'} \frac{\mathrm{d}t_1\,\mathrm{d}t_2\,\mathrm{d}t_3}{(1+\|t_1-t_2\|)^{\gamma(q-k_3)}(1+\|t_1-t_3\|)^{\gamma(q-k_2)}(1+\|t_2-t_3\|)^{\gamma(q-k_1)}}\,.
\end{aligned}
$$

Set

$$
A_q(k_1,k_2,k_3) := \frac{\sqrt{(k_1-1)!(k_2-1)!(k_3-1)!}}{(k_1k_2k_3)^{\frac{1}{12}}(q-k_1)!(q-k_2)!(q-k_3)!}, \quad k_1+k_2+k_3 = 2q.
$$

Consider the decomposition,

$$
\begin{aligned}
|V_{3,\le N_{T,T'}}| \le\ & 4c_\beta^3\,|T| \sum_{q=4}^{N_{T,T'}} \Big(\sum_{k_3=1}^{\lfloor q/4\rfloor} + \sum_{k_3=\lfloor q/4\rfloor+1}^{q} \Big) \sum_{\substack{k_1,k_2\in\{1,\dots,q\}\\ k_1+k_2+k_3=2q}} A_q(k_1,k_2,k_3) \\
& \times \int_T\int_T\int_{T'} \frac{\mathrm{d}t_1\,\mathrm{d}t_2\,\mathrm{d}t_3}{(1+\|t_1-t_2\|)^{\gamma(q-k_3)}(1+\|t_1-t_3\|)^{\gamma(q-k_2)}(1+\|t_2-t_3\|)^{\gamma(q-k_1)}} \\
=:\ & 4c_\beta^3\,|T|\big(V_{3,1}+V_{3,2}\big).
\end{aligned} \tag{29}
$$

First, we consider $V_{3,1}$, *i.e.* the set $\{1 \le k_3 \le \lfloor q/4\rfloor\}$. Straightforward computations and the fact that $k_3 = 2q-k_1-k_2$, lead to

$$
V_{3,1} \le |T| \sum_{q=4}^{N_{T,T'}} \sum_{k_3=1}^{\lfloor q/4\rfloor} \frac{1}{(\mathrm{dist}(T,T'))^{\gamma k_3}} \sum_{\substack{k_1,k_2\in\{1,\dots,q\}\\ k_1+k_2=2q-k_3}} A_q(k_1,k_2,k_3) \int_T\int_T \frac{\mathrm{d}t_1\,\mathrm{d}t_2}{(1+\|t_1-t_2\|)^{\gamma(q-k_3)}}. \tag{30}
$$

For the integral in (30), after two successive changes of variables we get, for all $Q>1$ that

$$
\begin{aligned}
\int_T\int_T \frac{\mathrm{d}t_1\,\mathrm{d}t_2}{(1+\|t_1-t_2\|)^Q} &= \int_{\mathbb{R}} \mathbf{1}_{t_1\in T} \int_{\mathbb{R}} \frac{\mathbf{1}_{u\in T-t_1}}{(1+\|u\|)^Q}\mathrm{d}u\mathrm{d}t_1 = \int_T \Big(\int_0^{2\pi}\int_{\mathbb{R}_+} \frac{\mathbf{1}_{re^{i\theta}\in T-t_1}}{(1+r)^Q} r\mathrm{d}r\mathrm{d}\theta \Big)\mathrm{d}t_1 \\
&\le 2\pi|T| \int_0^\infty \frac{r\mathrm{d}r}{(1+r)^Q} \le C|T|\frac{1}{Q^2}, \quad \forall Q>1,
\end{aligned} \tag{31}
$$

where the last inequality follows from an integration by part and C is a positive constant. Next, for all

$k_3 \le \lfloor q/4 \rfloor$, it holds

$$\begin{aligned}
\sum_{\substack{k_1,k_2\in\{1,\dots,q\}\\ k_1+k_2=2q-k_3}} A_q(k_1,k_2,k_3) &= \frac{\sqrt{(k_3-1)!}}{k_3^{\frac{1}{12}}(q-k_3)!} \sum_{\substack{k_1,k_2\in\{1,\dots,q\}\\ k_1+k_2=2q-k_3}} \frac{\sqrt{(k_1-1)!(k_2-1)!}}{(k_1k_2)^{\frac{1}{12}}(q-k_1)!(q-k_2)!} \\
&\le 2\frac{\sqrt{(k_3-1)!}}{k_3^{\frac{1}{12}}(q-k_3)!} \sum_{k=q-k_3}^{q} \frac{\sqrt{(k-1)!(2q-k-k_3-1)!}}{(k(2q-k-k_3))^{\frac{1}{12}}(q-k)!(k+k_3-q)!} \\
&= 2\frac{\sqrt{(k_3-1)!}}{k_3^{\frac{1}{12}}(q-k_3)!} \sum_{\ell=0}^{k_3} \frac{\sqrt{(\ell+q-k_3-1)!(q-\ell-1)!}}{((\ell+q-k_3)(q-\ell))^{\frac{1}{12}}(k_3-\ell)!\ell!} \\
&\le 2\Big(\frac{4}{3}\Big)^{\frac{1}{12}} \frac{\sqrt{(k_3-1)!(q-k_3-1)!(q-1)!}}{q^{\frac{1}{6}}k_3^{\frac{1}{12}}(q-k_3)!k_3!} \sum_{\ell=0}^{k_3}\binom{k_3}{\ell} \le 2\Big(\frac{4}{3}\Big)^{\frac{7}{12}} \frac{2^{k_3}}{q^{1+\frac{1}{6}}k_3^{\frac{7}{12}}}\sqrt{\binom{q}{k_3}}, \qquad (32)
\end{aligned}$$

where we used that $k_3 \le \lfloor q/4 \rfloor$ and that $\ell \mapsto \sqrt{(\ell+q-k_3-1)!(q-\ell-1)!}$ is symmetric and maximal for $\ell = 0$ (or $\ell = k_3$). Injecting (31) and (32) in (30) and using that $1 \le k_3 \le \lfloor q/4 \rfloor$, lead –for a positive constant C whose value may change from line to line– to

$$V_{3,1} \le C|T|^2 \sum_{q=4}^{N_{T,T'}} \frac{1}{q^{3+\frac{1}{6}}} \sum_{k_3=1}^{\lfloor q/4 \rfloor} \frac{2^{k_3}}{(\mathrm{dist}(T,T'))^{\gamma k_3}} \sqrt{\binom{q}{k_3}}.$$

Set $\eta_{T,T'} := \big(2/(\mathrm{dist}(T,T'))^{\gamma}\big)$ and note that $u_k : k \mapsto \eta_{T,T'}^k \sqrt{\binom{q}{k}}$ is decreasing and bounded by $\sqrt{q}$ iff

$$\frac{u_{k+1}}{u_k} = \eta_{T,T'}\sqrt{\frac{q+1}{k+1}-1} \le 1 \quad \Longleftrightarrow \quad k \ge \frac{q+1}{\eta_{T,T'}^2+1}\eta_{T,T'}^2 - 1$$

which always holds if $q \le (\eta_{T,T'})^{-2}$. Finally, fix $N_{T,T'} := \lfloor (\eta_{T,T'})^{-2} \rfloor$, note that we have $N_{T,T'} \to \infty$ as $\mathrm{dist}(T,T') \to \infty$. It follows that

$$V_{3,1} \le C\frac{|T|^2}{(\mathrm{dist}(T,T'))^{\gamma}} \sum_{q=4}^{N_{T,T'}} \frac{q\sqrt{q}}{q^{3+\frac{1}{6}}} \le C\frac{|T|^2}{(\mathrm{dist}(T,T'))^{\gamma}} \sum_{q=4}^{\infty} q^{-\frac{5}{3}} = o\big(|T|^2\big). \qquad (33)$$

Second, we study the set $\{\lfloor q/4 \rfloor + 1 \le k_3 \le q\}$, similarly we get

$$V_{3,2} \le |T| \sum_{q=4}^{N_{T,T'}} \sum_{k_3=\lfloor q/4 \rfloor+1}^{q} \sum_{\substack{k_1,k_2\in\{1,\dots,q\}\\ k_1+k_2+k_3=2q}} \frac{A_q(k_1,k_2,k_3)}{(\mathrm{dist}(T,T'))^{\gamma k_3}} \int_T \int_T \frac{\mathrm{d}t_1\,\mathrm{d}t_2}{(1+\|t_1-t_2\|)^{\gamma(q-k_3)}}.$$

Note that $(k_1,k_2,k_3,$ subject to $k_1+k_2+k_3 = 2q) \mapsto A_q(k_1,k_2,k_3)$ is maximal for $k_1 \asymp k_2 \asymp k_3 \asymp \lfloor 2q/3 \rfloor$, and the Stirling formula gives $A_q(\lfloor 2q/3 \rfloor, \lfloor 2q/3 \rfloor, \lfloor 2q/3 \rfloor) = O(q^{-1}2^q)$. Moreover, $\mathrm{Card}\big((k_1,k_2,k_3),\, 1 \le k_1,k_2 \le q,\, k_3 \ge \lfloor q/4 \rfloor,\, k_1+k_2+k_3 = 2q\big) \le q^2$. It follows that for some positive constant C,

$$V_{3,2} \le C\,|T| \int_{\mathbb{R}^2} \frac{\mathrm{d}t_1\,\mathrm{d}t_2}{(1+\|t_1-t_2\|)^{\gamma}} \sum_{q=4}^{N_{T,T'}} \frac{2^q}{q} q^2 \frac{1}{(\mathrm{dist}(T,T'))^{\gamma q/4}}. \qquad (34)$$

It follows that for $\mathrm{dist}(T,T') > 2^{4/\gamma}$, $V_{3,2} = o(|T|)$. Observe that the condition for convergence of this term depends on γ: the larger γ is the weakest the condition on $\mathrm{dist}(T,T')$ is. Gathering (33) and (34) in (29), we derive that $V_{3,\leq N_{T,T'}} = o(|T|^3)$, this together with $V_{3,>N_{T,T'}} = o(|T|)$ implies that $V_3 = o(|T|^3)$.

Control of V_4. Similarly to V_3, we rely on the diagram formula and the following decomposition

$$\begin{aligned} V_4 &= \left(\sum_{q\geq 4}^{N_{T,T'}} + \sum_{q=N_{T,T'}+1}^{\infty} \right) \sum_{(k_1,k_2,k_3,k_4)\in\mathbb{N}\setminus\{0\}} \frac{\beta_{k_1}(s_{u_1})\beta_{k_2}(s_{u_2})\beta_{k_3}(s_{u_3})\beta_{k_4}(s_{u_4})}{k_1!k_2!k_3!k_4!} \\ &\qquad \times \int_T \int_T \int_{T'} \int_{T'} \mathbb{E}[H_{k_1}(G(t_1))H_{k_2}(G(t_2))H_{k_3}(G(t_3))H_{k_4}(G(t_4))]\,\mathrm{d}t_1\,\mathrm{d}t_2\,\mathrm{d}t_3\,\mathrm{d}t_4 \\ &= V_{4,\leq N_{T,T'}} + V_{4,>N_{T,T'}}, \end{aligned}$$

for some positive integer $N_{T,T'}$ depending on T and T' and such that $N_{T,T'} \to \infty$ as $\mathrm{dist}(T,T') \to \infty$. Using similar arguments as for $V_{3,>N_{T,T'}}$, we derive that $V_{4,>N_{T,T'}} = O(|T|^2)$ as $\mathrm{dist}(T,T') \to \infty$.
We focus on $V_{4,\leq N_{T,T'}}$ and compute $T_{k_1,k_2,k_3,k_4} := \mathbb{E}[H_{k_1}(G_1)H_{k_2}(G_2)H_{k_3}(G_3)H_{k_4}(G_4)]$ for $k_j \geq 1$, $j \in \{1,2,3,4\}$ and (G_1,G_2,G_3,G_4) a standard Gaussian (see Taqqu (1977) Definition 3.1) with $\rho_{i,j} := \mathbb{E}[G_iG_j] = \rho_{j,i}$ such that $|\rho_{i,j}| \leq 1$, for $1 \leq i,j \leq 4$. The diagram formula –taking into account that $\rho_{i,j} = \rho_{j,i}$, which comes down to multiplying the one given in Taqqu (1977), Lemma 3.2, by 2^q (see also proof of Lemma 10.7 in Azaïs and Wschebor (2009)– gives

$$T_{k_1,k_2,k_3,k_4} = \begin{cases} \frac{k_1!k_2!k_3!k_4!}{q!} \displaystyle\sum_{\mathcal{I}(k_1,k_2,k_3,k_4)} \rho_{i_1,j_1}\ldots\rho_{i_q,j_q} & \text{if } k_1+\ldots+k_4 = 2q,\ 1 \leq k_1,k_2,k_3,k_4 \leq q, \\ 0 & \text{otherwise,} \end{cases} \tag{35}$$

where the set of indices $\mathcal{I}(k_1,k_2,k_3,k_4)$ is the set of all indices $(i_1,j_1,\ldots,i_q,j_q)$ such that

i+ii) $((i_1,j_1),\ldots,(i_q,j_q)) \in \{(1,2),(1,3),(1,4),(2,3),(2,4),(3,4)\}^q =: \mathcal{I}_{pair}{}^q$,

iii) there are k_1 indices 1, k_2 indices 2, k_3 indices 3 and k_4 indices 4.

For $q \in \mathbb{N}$, $q \geq 4$ define the set of indices $\mathcal{J}_4(q) = \{(k_1,k_2,k_3,k_4) \in \{1,\ldots,q\}^4,\ k_1+k_2+k_3+k_4 = 2q\}$. formulae (35) and (26) lead to, for a positive constant C whose value may change from line to line,

$$\begin{aligned} V_{4,\leq N_{T,T'}} &= \sum_{q=4}^{N_{T,T'}} \sum_{(k_1,k_2,k_3,k_4)\in\mathcal{J}_4(q)} \frac{\beta_{k_1}(s_{u_1})\beta_{k_2}(s_{u_2})\beta_{k_3}(s_{u_3})\beta_{k_4}(s_{u_4})}{k_1!k_2!k_3!k_4!} T_{k_1,k_2,k_3,k_4} \\ &\leq C \sum_{q=4}^{N_{T,T'}} \frac{1}{q!} \sum_{(k_1,k_2,k_3,k_4)\in\mathcal{J}_4(q)} \frac{\sqrt{(k_1-1)!(k_2-1)!(k_3-1)!(k_4-1)!}}{(k_1k_2k_3k_4)^{\frac{1}{12}}} \\ &\qquad \times \sum_{\mathcal{I}(k_1,k_2,k_3,k_4)} \int_T \int_T \int_{T'} \int_{T'} \prod_{a\in\mathcal{I}_{pair}} \left(1+\|t_i-t_j\|\right)^{-\gamma q_a} \mathrm{d}t_1\,\mathrm{d}t_2\,\mathrm{d}t_3\,\mathrm{d}t_4, \end{aligned}$$

where q_a for is the number of occurrences of the pair a and $\mathcal{I}(k_1,k_2,k_3,k_4)$ reduces to the set of indices

such that

$$\begin{cases} q_{(1,2)}+q_{(1,3)}+q_{(1,4)}+q_{(2,3)}+q_{(2,4)}+q_{(3,4)}=q, \\ q_{(1,2)}+q_{(1,3)}+q_{(1,4)}=k_1, \\ q_{(1,2)}+q_{(2,3)}+q_{(2,4)}=k_2, \\ q_{(1,3)}+q_{(2,3)}+q_{(3,4)}=k_3, \\ q_{(1,4)}+q_{(2,4)}+q_{(3,4)}=k_4. \end{cases} \tag{36}$$

Denote $\mathcal{I}_{pair}(q) = \big\{q_a,\, a\in\mathcal{I}_{pair},\, \sum_{a\in\mathcal{I}_{pair}} q_a = q,\, \sum_{(i,j)} q_{(i,j)}\mathbf{1}_{\{i=l\}\cup\{j=l\}} = k_l\big\}$, the latter can be rewritten as

$$\begin{aligned} V_{4,\le N_{T,T'}} \le\, & C\sum_{q=4}^{N_{T,T'}}\frac{1}{q!}\sum_{\mathcal{I}_{pair}(q)}\frac{\sqrt{(k_1-1)!(k_2-1)!(k_3-1)!(k_4-1)!}}{(k_1k_2k_3k_4)^{\frac{1}{12}}} \\ & \binom{q}{q_{(1,2)},q_{(1,3)},q_{(1,4)},q_{(2,3)},q_{(2,4)},q_{(3,4)}}\int_T\int_T\int_{T'}\int_{T'}\prod_{a\in\mathcal{I}_{pair}}\big(1+\|t_i-t_j\|\big)^{-\gamma q_a}\,\mathrm{d}t_1\,\mathrm{d}t_2\,\mathrm{d}t_3\,\mathrm{d}t_4 \\ =\, & C\sum_{q=4}^{N_{T,T'}}\sum_{\mathcal{I}_{pair}(q)}\frac{\sqrt{(k_1-1)!(k_2-1)!(k_3-1)!(k_4-1)!}}{(k_1k_2k_3k_4)^{\frac{1}{12}}q_{(1,2)}!q_{(1,3)}!q_{(1,4)}!q_{(2,3)}!q_{(2,4)}!q_{(3,4)}!} \\ & \int_T\int_T\int_{T'}\int_{T'}\prod_{a\in\mathcal{I}_{pair}}\big(1+\|t_i-t_j\|\big)^{-\gamma q_a}\,\mathrm{d}t_1\,\mathrm{d}t_2\,\mathrm{d}t_3\,\mathrm{d}t_4. \end{aligned}$$

Similarly to $V_{3,\le N_{T,T'}}$, we decompose this majorant of $V_{4,\le N_{T,T'}}$ in $V_{4,1}+V_{4,2}$ according to $\{q_{(1,2)}+q_{(3,4)}\le\lfloor 3q/4\rfloor\}$ (which plays the same role as $q-k_3$ in $V_{3,\le N_{T,T'}}$) and its complementary set.
First, we study the set $\{q_{(1,2)}+q_{(3,4)}\le\lfloor 3q/4\rfloor\}$, where $q_{(1,3)}+q_{(1,4)}+q_{(2,3)}+q_{(2,4)}\ge\frac{q}{4}$, it follows

$$\begin{aligned} V_{4,1} \le\, & C\left(\int_T\int_T\frac{\mathrm{d}t_1\mathrm{d}t_2}{(1+\|t_1-t_2\|)^\gamma}\right)^2\sum_{q=4}^{N_{T,T'}}\frac{1}{\big(\mathrm{dist}(T,T')\big)^{\gamma q/4}} \\ & \times\sum_{\substack{\mathcal{I}_{pair}(q)\\ q_{(1,2)}+q_{(3,4)}\le\lfloor 3q/4\rfloor}}\frac{\sqrt{(k_1-1)!(k_2-1)!(k_3-1)!(k_4-1)!}}{(k_1k_2k_3k_4)^{\frac{1}{12}}q_{(1,2)}!q_{(1,3)}!q_{(1,4)}!q_{(2,3)}!q_{(2,4)}!q_{(3,4)}!} \\ \le\, & C\left(\int_T\int_T\frac{\mathrm{d}t_1\mathrm{d}t_2}{(1+\|t_1-t_2\|)^\gamma}\right)^2\sum_{q=4}^{N_{T,T'}}\frac{1}{\big(\mathrm{dist}(T,T')\big)^{\gamma q/4}}q^5\frac{\left(\frac{3q}{6}-1\right)!^2}{\left(\frac{q}{6}\right)!^6}, \end{aligned} \tag{37}$$

where we used that $k_\cdot\ge 1$, the cardinality of $\mathcal{I}_{pair}(q)$ is bounded by q^5 and that the ratio in (37) is maximal for $q_a=\lfloor q/6\rfloor$, $\forall a\in\mathcal{I}_{pair}$. Using that $\sqrt{2\pi m}\big(\frac{m}{e}\big)^m\le m!\le 2\sqrt{2\pi m}\big(\frac{m}{e}\big)^m$ provides the bound $\big(\frac{3q}{6}\big)!^2/\big(\frac{q}{6}\big)!^6\le C3^q/q^2$ and we get for $\mathrm{dist}(T,T')>3^{4/\gamma}$ that

$$V_{4,1}\le C\left(\int_{\mathbb{R}^2}\frac{\mathrm{d}t_1\mathrm{d}t_2}{(1+\|t_1-t_2\|)^\gamma}\right)^2\sum_{q=4}^{+\infty}q\frac{3^q}{\big(\mathrm{dist}(T,T')\big)^{\gamma q/4}}=O(1). \tag{38}$$

Second, consider the set $\{q_{(1,2)}+q_{(3,4)} > \lfloor 3q/4 \rfloor\}$,

$$V_{4,2} \leq C \sum_{q=4}^{N_{T,T'}} \sum_{\substack{\mathcal{I}_{pair}(q) \\ q_{(1,2)}+q_{(3,4)}>\lfloor 3q/4 \rfloor}} \frac{\sqrt{(k_1-1)!(k_2-1)!(k_3-1)!(k_4-1)!}}{(k_1k_2k_3k_4)^{\frac{1}{12}} q_{(1,2)}!q_{(1,3)}!q_{(1,4)}!q_{(2,3)}!q_{(2,4)}!q_{(3,4)}!} \int_T \int_T \int_{T'} \int_{T'} \prod_{a\in\mathcal{I}_{pair}} \left(1+\|t_i-t_j\|\right)^{-\gamma q_a} \mathrm{d}t_1\,\mathrm{d}t_2\,\mathrm{d}t_3\,\mathrm{d}t_4.$$

Note that, if $q_{(1,2)}+q_{(3,4)} > \lfloor 3q/4 \rfloor$, it follows that $\max\{q_{(1,2)}, q_{(3,4)}\} > \lfloor 3q/8 \rfloor$, then using (36) we derive that on this set $(k_1k_2k_3k_4)^{-1/12} \leq Cq^{-1/6}$, for some positive constant C. Next, we decompose $V_{4,2}$ according to the values of $k = q_{(1,3)}+q_{(1,4)}+q_{(2,3)}+q_{(2,4)} \leq \lfloor q/4 \rfloor$ and use Assumption ($\mathcal{A}1$), (31) and (36) to get

$$\begin{aligned} V_{4,2} \leq\ & C|T|^2 \sum_{q=4}^{N_{T,T'}} q^{-1/6} \sum_{k=0}^{\lfloor q/4 \rfloor} \frac{1}{(\mathrm{dist}(T,T'))^{\gamma k}} \sum_{q_{(1,3)}+q_{(1,4)}+q_{(2,3)}+q_{(2,4)}=k} \frac{1}{q_{(1,3)}!q_{(1,4)}!q_{(2,3)}!q_{(2,4)}!} \\ & \times \sum_{q_{(1,2)}=1}^{q-k-1} \frac{\sqrt{(q_{(1,2)}+q_{(1,3)}+q_{(1,4)}-1)!(q_{(1,2)}+q_{(2,3)}+q_{(2,4)}-1)!}}{q_{(1,2)}!q_{(1,2)}^2} \\ & \times \frac{\sqrt{(q_{(1,3)}+q_{(2,3)}+q-k-q_{(1,2)}-1)!(q_{(1,4)}+q_{(2,4)}+q-k-q_{(1,2)}-1)!}}{(q-k-q_{(1,2)})!(q-k-q_{(1,2)})^2}, \end{aligned}$$

where the constant C contains $\int_{\mathbb{R}^2}(1+\|t-s\|)^{-2}\mathrm{d}t\mathrm{d}s$. Observe that the function in $q_{(1,2)}$ in the last summand is symmetric with respect to $(q-k)/2$ and is maximal for $q_{(1,2)} \in \{1, q-k-1\}$. It follows that

$$\begin{aligned} V_{4,2} \leq\ & C|T|^2 \sum_{q=4}^{N_{T,T'}} q^{-1/6} \sum_{k=0}^{\lfloor q/4 \rfloor} \frac{1}{(\mathrm{dist}(T,T'))^{\gamma k}} \sum_{q_{(1,3)}+q_{(1,4)}+q_{(2,3)}+q_{(2,4)}=k} \frac{1}{q_{(1,3)}!q_{(1,4)}!q_{(2,3)}!q_{(2,4)}!} \\ & \times \frac{\sqrt{(q_{(1,3)}+q_{(1,4)})!(q_{(2,3)}+q_{(2,4)})!(q_{(1,3)}+q_{(2,3)}+q-k-2)!(q_{(1,4)}+q_{(2,4)}+q-k-2)!}}{(q-k-1)!(q-k-1)}. \end{aligned}$$

Considering the function in $\left(q_{(1,3)}, q_{(1,4)}, q_{(2,3)}, q_{(2,4)}\right)$ under the square root in the last display, it is easy —considering all possible cases— to derive that it is maximal at $(k,0,0,0)$ (the maximum is not unique). We obtain

$$\begin{aligned} V_{4,2} \leq\ & C|T|^2 \sum_{q=4}^{N_{T,T'}} q^{-\frac{1}{6}} \sum_{k=0}^{\lfloor q/4 \rfloor} \frac{1}{(\mathrm{dist}(T,T'))^{\gamma k}k!} \sum_{\substack{q_{(1,3)}+q_{(1,4)}+ \\ q_{(2,3)}+q_{(2,4)}=k}} \frac{k!}{q_{(1,3)}!q_{(1,4)}!q_{(2,3)}!q_{(2,4)}!} \frac{\sqrt{k!(q-2)!(q-k-2)!}}{(q-k-1)!(q-k-1)} \\ =\ & C|T|^2 \sum_{q=4}^{N_{T,T'}} q^{-\frac{1}{6}} \sum_{k=0}^{\lfloor q/4 \rfloor} \frac{4^k}{(\mathrm{dist}(T,T'))^{\gamma k}} \frac{\sqrt{(q-2)!}}{(q-k-1)^2\sqrt{k!(q-k-2)!}}, \end{aligned}$$

where we used the multinomial theorem. Therefore, we derive that

$$V_{4,2} \leq C|T|^2 \sum_{q=4}^{N_{T,T'}} q^{-2-\frac{1}{6}} \sum_{k=0}^{\lfloor q/4 \rfloor} \frac{4^k}{(\mathrm{dist}(T,T'))^{\gamma k}} \sqrt{\binom{q}{k}}$$

Finally, as for $V_{3,2}$ if we set $\eta_{T,T'} := \left(4/(\mathrm{dist}(T,T'))^{\gamma}\right)$ the function $k \mapsto \eta_{T,T'}^{k}\sqrt{\binom{q}{k}}$ is decreasing if $q \leq (\eta_{T,T'})^{-2}$. Fix $N_{T,T'} := \lfloor (\eta_{T,T'})^{-2} \rfloor$, note that we have $N_{T,T'} \to \infty$ as $\mathrm{dist}(T,T') \to \infty$. It follows that

$$V_{4,2} \leq C|T|^2 \sum_{q=4}^{N_{T,T'}} \frac{q}{q^{2+\frac{1}{6}}} \leq C|T|^2. \tag{39}$$

Gathering (38) and (39) show that $V_{4,\leq N_{T,T4}} = O(|T|^2)$ and finally that $V_4 = O(|T|^2)$.
Gathering the control of four terms, V_0 to V_4, lead to the announced result in Proposition 3.1. □

A.4 Elements to establish Conjecture 3.1

Following the same structure as for the proof of Proposition 3.1 should lead to the result. Already in the proof of Proposition 3.1 managing the terms V_3 and V_4 was lengthly and technical, in the case of the Euler characteristic the difficulty increases dramatically. We give the elements that could be used to establish the result in a similar pattern as for the proof of Proposition 3.1, but we do not pursue in details the study of all the terms involved.

Modified Euler characteristic As we focus on domain T such that $T \nearrow \mathbb{R}^2$, without loss of generality we can consider in the sequel the modified Euler characteristic $\widetilde{C}_0^{/T}(X,u)$ as in (4) instead of $C_0^{/T}(X,u)$. Roughly speaking, we neglect boundary terms depending on the behavior of $\mathcal{L}_0(X,u,T)$ on ∂T (see Sections 1.2 and 2.3 in Estrade and León (2016)).
More precisely, we follow the presentation of Adler and Taylor (2007) Section 9.4, inspired by Morse's theorem, to give the following decomposition of the Euler characteristic of the excursion set $E_X(u)$,

$$\begin{aligned} C_0^{/T}(X,u) := \frac{\mathcal{L}_0(X,u,T)}{|T|} &= \frac{1}{|T|}\left(\sum_{l\in\{0,1\}} \sum_{J\in\partial_l T} \mathcal{L}_0(X,u,J) + \mathcal{L}_0(X,u,\mathring{T}) \right) \\ &= \sum_{l\in\{0,1\}} \sum_{J\in\partial_l T} \frac{\mathcal{L}_0(X,u,J)}{|T|} + \widetilde{C}_0^{/T}(X,u), \end{aligned} \tag{40}$$

where $\partial_l T$ denotes the collection of all the l-dimensional faces of T. In particular $\partial_2 T$ only contains the interior of T, *i.e.*, $\mathring{T}$, $\partial_1 T$ is the union of the interiors of the 1-dimensional faces of T and $\partial_0 T$ is the union of the 4 vertices of the rectangle T (see Section 4.6 in Adler and Taylor (2007)). Therefore, the first term in (40) vanishes as $|T| \to \infty$, in the remaining of the proof we focus on $\widetilde{C}_0^{/T}(X,u)$ for which there is an Itô-Wiener chaos decomposition.

Itô-Wiener chaos decomposition for $\widetilde{C}_0^{/T}(X,u)$ Let X be a Gaussian random field satisfying Assumption ($\mathcal{A}0$), denote the gradient of X by $\nabla X := \begin{pmatrix} X_1 \\ X_2 \end{pmatrix}$ and the Hessian matrix of X by $\nabla^2(X) := \begin{pmatrix} X_{1,1} & X_{1,2} \\ X_{1,2} & X_{2,2} \end{pmatrix}$. We now deal with the 6-dimensional Gaussian vector $\mathbf{X}$ defined for any $t = (t_1,t_2) \in \mathbb{R}^2$ we write the coordinates of $\mathbf{X}$ such that $\mathbf{X}(t_1,t_2) := (\mathbf{X}_1,\mathbf{X}_2,\mathbf{X}_3,\mathbf{X}_4,\mathbf{X}_5,\mathbf{X}_6)(t_1,t_2)$ with $\mathbf{X}_3 = X_{1,2}$, $\mathbf{X}_4 = X_{1,1}$, $\mathbf{X}_5 = X_{2,2}$ and $\mathbf{X}_6 = X$ (see also Estrade and León (2016)).
By using the stationarity and the isotropy of the considered Gaussian field, it is well know that for any fixed t, $X(t)$ and $\nabla X(t)$ are independent, as well as $\nabla X(t)$ and $\nabla^2 X(t)$. Moreover, since X is isotropic, for any fixed t, $X_1(t)$ and $X_2(t)$ are independent (see Adler and Taylor (2007), Section 5.5). Then, by

applying Equations (5.5.5), (5.5.6) and (5.5.7) in Adler and Taylor (2007) and using the fact that all the odd-ordered derivatives of r are identically zero, it is possible to derive all the elements of the covariance matrix of $\mathbf{X}$ in our non-unit variance framework:

$$\Sigma^{\mathbf{X}} = \begin{pmatrix} \frac{\lambda}{\sigma_g^2} & 0 & 0 & 0 & 0 & 0 \\ 0 & \frac{\lambda}{\sigma_g^2} & 0 & 0 & 0 & 0 \\ 0 & 0 & \frac{\mu}{3\sigma_g^2} & 0 & 0 & 0 \\ 0 & 0 & 0 & \frac{\mu}{\sigma_g^2} & \frac{\mu}{3\sigma_g^2} & \frac{-\lambda}{\sigma_g^2} \\ 0 & 0 & 0 & \frac{\mu}{3\sigma_g^2} & \frac{\mu}{\sigma_g^2} & \frac{-\lambda}{\sigma_g^2} \\ 0 & 0 & 0 & \frac{-\lambda}{\sigma_g^2} & \frac{-\lambda}{\sigma_g^2} & \sigma_g^2 \end{pmatrix}.$$

The covariance function of $\Gamma^{\mathbf{X}}(\cdot)$ of $\mathbf{X}$ takes values in the set of symmetric 6×6 matrices with elements equal to r or a derivative of r. Choose Λ a 6×6 matrix such that $\Lambda\Lambda^t = \Sigma^{\mathbf{X}}$, where Λ^t denotes the transpose of Λ. We can thus write, for any fixed $t \in \mathbb{R}^2$, $\mathbf{X}(t) = \Lambda\, Y(t)$ with $Y(t)$ a 6-dimensional centered Gaussian vector with variance I_6 and covariance function $\Gamma^{\mathbf{Y}}(t)$ given by $\Gamma^{\mathbf{Y}}(t) = \Lambda^{-1}\Gamma^{\mathbf{X}}(t)(\Lambda^{-1})^t$. As in Estrade and León (2016), one can consider

$$\Lambda = \begin{pmatrix} \sqrt{\frac{\lambda}{\sigma_g^2}} I_2 & 0 \\ 0 & \Lambda_2 \end{pmatrix} \quad \text{where} \quad \Lambda_2 = \begin{pmatrix} a & 0 & 0 & 0 \\ 0 & b & 0 & 0 \\ 0 & d & c & 0 \\ 0 & A & B & \alpha \end{pmatrix} \tag{41}$$

where $a = \sqrt{\frac{\mu}{3\sigma_g^2}}$, $b = \sqrt{\frac{\mu}{\sigma_g^2}}$, $c = \sqrt{\frac{8\mu}{9\sigma_g^2}}$, $d = \sqrt{\frac{\mu}{9\sigma_g^2}}$, $A = -\frac{\lambda}{\sigma_g\sqrt{\mu}}$, $B = -\frac{\lambda}{\sigma_g\sqrt{2\mu}}$, $\alpha = \frac{\sqrt{\frac{2\mu}{3} - \frac{\lambda^2}{\sigma_g^2}}}{\sqrt{\frac{2\mu}{3}}}$.
Under Assumption ($\mathcal{A}2$), one can write the following Itô-Wiener chaos expansion for $\widetilde{C}_0^{/T}(X, u)$:

$$\widetilde{C}_0^{/T}(X, u) = \frac{1}{|T|} \sum_{q=0}^{+\infty} \sum_{\mathbf{n} \in \mathbb{N}^6 : |\mathbf{n}| = q} a(\mathbf{n}, u) \int_T \widetilde{H}_{\mathbf{n}}(Y(t))\mathrm{d}t, \tag{42}$$

with $\mathbf{n} = (n_1, n_2, n_3, n_4, n_5, n_6)$, $n_i \in \mathbb{N}$, $|\mathbf{n}| = n_1 + n_2 + n_3 + n_4 + n_5 + n_6$ and for $y = (y_1, y_2, y_3, y_4, y_5, y_6)$ $\widetilde{H}_{\mathbf{n}}(y) = \prod_{1 \le j \le 6} H_{n_j}(y_j)$ where H_n is the n-th Hermite polynomial (see *e.g.*, Proposition 1.3 in Estrade and León (2016)).

On the coefficients $a(\mathbf{n}, u)$ It holds that

$$a(\mathbf{0}, u) = \frac{\sigma_g^2}{2\pi\lambda} \varphi(s_u)\, \frac{\lambda^2}{\sigma_g^4} s_u. \tag{43}$$

Indeed, the mean of $\widetilde{C}_0^{/T}(X, u)$ is its projection into the 0-th Itô-Wiener chaos, *i.e.*, $\mathbb{E}[\widetilde{C}_0^{/T}(X, u)] = C_0^*(X, u) = \frac{a}{(2\pi)^{3/2}} \exp\{-\frac{1}{2}s_u^2\} s_u$ (see (7)). Moreover, $a(\mathbf{n}, u) = 0$ as soon as n_1 or n_2 is odd, or $n_3 \neq 0$ or $n_3 \neq 2$. Furthermore according to the Mehler's Formula (see Lemma 10.7 in Azaïs and Wschebor (2009)),

$$\text{if } |\mathbf{n}| \neq |\mathbf{m}| \quad \text{then} \quad \mathrm{Cov}(\widetilde{H}_{\mathbf{n}}(Y(s)), \widetilde{H}_{\mathbf{m}}(Y(t))) = 0.$$

Under Assumption ($\mathcal{A}2$) one can get, for $|\mathbf{n}| = |\mathbf{m}| = q$,

$$\mathrm{Cov}(\widetilde{H}_{\mathbf{n}}(Y(0)), \widetilde{H}_{\mathbf{m}}(Y(t))) \leq K M_r^q(t) \tag{44}$$

for some positive constant K, where M_r is defined in Assumption ($\mathcal{A}2$).
Identifying any symmetric matrix of size 2×2 with the 3−dimensional vector containing the coefficients on and above the diagonal and write $\widetilde{det}$ the associated determinant map. Then, one can get

$$\sum_{\mathbf{n}\in\mathbb{N}^6:|\mathbf{n}|=q} a(\mathbf{n}, u)^2 \mathbf{n}! \leq C\, q^2 \|f_u \cdot \Lambda_2\|^2, \tag{45}$$

with Λ_2 as in (41) and $(y, z) \in \mathbb{R}^3 \times \mathbb{R} \mapsto f_u(y, z) = \widetilde{det}(y) 1_{[u,+\infty)}(z)$, see Estrade and León (2016).

How to control the fourth moment of $\widetilde{C}_0$ Denote $T_1 = T_2 := T$ and $T_3 = T_4 := T'$ and use that $|T| = |T'|$. Using (42) we get (having $\widetilde{C}_0^{/T}(X, u) := \widetilde{C}_0(X, u, T)$)

$$\begin{aligned} M_{4,0} :&= |T|^4\, \mathbb{E}[\widetilde{C}_0(X, u_1, T)\widetilde{C}_0(X, u_2, T)\widetilde{C}_0(X, u_3, T')\widetilde{C}_0(X, u_4, T')] \\ &= \sum_{q_1=0}^{+\infty}\sum_{q_2=0}^{+\infty}\sum_{q_3=0}^{+\infty}\sum_{q_4=0}^{+\infty} \sum_{\substack{\mathbf{n}(1)\in\mathbb{N}^6:\\ |\mathbf{n}(1)|=q_1}} \sum_{\substack{\mathbf{n}(2)\in\mathbb{N}^6:\\ |\mathbf{n}(2)|=q_2}} \sum_{\substack{\mathbf{n}(3)\in\mathbb{N}^6:\\ |\mathbf{n}(3)|=q_3}} \sum_{\substack{\mathbf{n}(4)\in\mathbb{N}^6:\\ |\mathbf{n}(4)|=q_4}} a(\mathbf{n}(1), u_1)a(\mathbf{n}(2), u_2)a(\mathbf{n}(3), u_3)a(\mathbf{n}(4), u_4) \\ &\quad \times \int_{T_1}\int_{T_2}\int_{T_3}\int_{T_4} \mathbb{E}[\widetilde{H}_{\mathbf{n}(1)}(Y(t_1))\widetilde{H}_{\mathbf{n}(2)}(Y(t_2))\widetilde{H}_{\mathbf{n}(3)}(Y(t_3))\widetilde{H}_{\mathbf{n}(4)}(Y(t_4))]\, \mathrm{d}t_1\, \mathrm{d}t_2\, \mathrm{d}t_3\, \mathrm{d}t_4. \end{aligned}$$

Similarly as for the case of the area, we decompose this fourth moment

$$M_{4,0} := V_0 + V_1 + V_2 + V_3 + V_4$$

where V_j are as in (27) replacing $\beta_n(s_{u_j})$ with $a(\mathbf{n}, \mathbf{0}, u_j)$, and $H_n(G(t_j))$ with $\widetilde{H}_{\mathbf{n}}(Y(t_j))$. The terms V_0, V_1 and V_2 can be treated readily with the tools introduced above. The terms that are computationally technical are V_3 and V_4 that require to apply the diagram formula in dimensions 18 and 24. Therefore, in the sequel we only present the result for V_0, V_1 and V_2, whose treatment is similar as for the area. We conjecture that V_3 and V_4 are $o(|T|^3)$ as for the area.

Control of V_0. It holds that $V_0 = |T|^4\, C_0^*(X, u_1)C_0^*(X, u_2)C_0^*(X, u_3)C_0^*(X, u_4)$ (see Equation (43)).

Control of V_1. We compute $\mathbb{E}[\widetilde{H}_{\mathbf{n}}(Y(t_j))]$, for that we use that Y is a 6-dimensional standard Gaussian vector, with independent coordinates, to get

$$\begin{aligned} \mathbb{E}[\widetilde{H}_{\mathbf{n}}(Y(t))] &= \mathbb{E}[H_{n_1}(Y_1(t))H_{n_2}(Y_2(t))H_{n_3}(Y_3(t))H_{n_4}(Y_4(t))H_{n_5}(Y_5(t))H_{n_6}(Y_6(t))] \\ &= \mathbb{E}[H_{n_1}(Y_1(t))]\, \mathbb{E}[H_{n_2}(Y_2(t))]\, \mathbb{E}[H_{n_3}(Y_3(t))]\, \mathbb{E}[H_{n_4}(Y_4(t))]\, \mathbb{E}[H_{n_5}(Y_5(t))]\, \mathbb{E}[H_{n_6}(Y_6(t))] = 0 \end{aligned}$$

using that if $|\mathbf{n}| \leq 1$, $\exists j \in \{1, 2, 3, 4, 5, 6\}$, $n_j \geq 1$ and the orthogonality of H_{n_j} with H_0 for the Gaussian measure. It follows that $V_1 = 0$.

Control of V_2. A slight generalization of Mehler's formula (see Lemma 10.7 in Azaïs and Wschebor (2009)) allows us to write that for any $\mathbf{n}(i_1)$ and $\mathbf{n}(i_2)$

$$\mathbb{E}[\widetilde{H}_{\mathbf{n}(i_1)}(Y(t_{i_1}))\widetilde{H}_{\mathbf{n}(i_2)}(Y(t_{i_2}))] = \mathrm{Cov}(\widetilde{H}_{\mathbf{n}(i_1)}(Y(t_{i_1})), \widetilde{H}_{\mathbf{n}(i_2)}(Y(t_{i_2}))),$$

where if $|\mathbf{n}(i_1)| \neq |\mathbf{n}(i_2)|$, it holds $\mathbb{E}[\widetilde{H}_{\mathbf{n}(i_1)}(Y(t_{i_1}))\widetilde{H}_{\mathbf{n}(i_2)}(Y(t_{i_2}))] = 0$ and if $|\mathbf{n}(i_1)| = |\mathbf{n}(i_2)| = q$, we get (see (44))

$$\mathrm{Cov}(\widetilde{H}_{\mathbf{n}(i_1)}(Y(t_{i_1})), \widetilde{H}_{\mathbf{n}(i_2)}(Y(t_{i_2}))) = \mathrm{Cov}(\widetilde{H}_{\mathbf{n}(i_1)}(Y(0)), \widetilde{H}_{\mathbf{n}(i_2)}(Y(t_{i_2} - t_{i_1}))) \leq K M_r^q(t_{i_2} - t_{i_1}),$$

where K is a positive constant. Then, it follows that

$$V_2 \leq K|T|^2 \Big(\sum_{j_1 \neq j_2 \in \mathcal{I}_{2,1}} + \sum_{j_1 \neq j_2 \in \mathcal{I}_{2,1}} \Big) a(\mathbf{0}, u_{j_1}) a(\mathbf{0}, u_{j_2}) \sum_{\substack{q=1 \\ i_1, i_2 \neq j_1, j_2}}^{+\infty} \sum_{\substack{\mathbf{n}(i_1) \in \mathbb{N}^6: \\ |\mathbf{n}(i_1)| = q}} \sum_{\substack{\mathbf{n}(i_2) \in \mathbb{N}^6: \\ |\mathbf{n}(i_2)| = q}} a(\mathbf{n}(i_1), u_{i_1}) a(\mathbf{n}(i_2), u_{i_2})$$
$$\times \int_{T_{i_1}} \int_{T_{i_2}} M_r(t_{i_1} - t_{i_2})^q \, \mathrm{d}t_{i_1} \, \mathrm{d}t_{i_2} := V_{2,1} + V_{2,2},$$

where $\mathcal{I}_{2,1} := \{(1,3),(1,4),(2,3),(2,4)\}$ and $\mathcal{I}_{2,2} := \{(1,2),(3,4)\}$. Using that on $\mathcal{I}_{2,1}$ the integration is made on distinct rectangles T and T', we get, denoting $g_s : u \mapsto \exp\{-\frac{1}{2}s_u^2\}s_u$,

$$|V_{2,1}| \leq \frac{a^2 K}{2\pi^3} \|g_s\|_\infty^2 |T|^2 \sum_{q=1}^{+\infty} \sum_{\substack{\mathbf{n}(i_1) \in \mathbb{N}^6: \\ |\mathbf{n}(i_1)| = q}} \sum_{\substack{\mathbf{n}(i_2) \in \mathbb{N}^6: \\ |\mathbf{n}(i_2)| = q}} a(\mathbf{n}(i_1), u_{i_1}) a(\mathbf{n}(i_2), u_{i_2}) \int_T \int_{T'} |M_r(t - t')|^q \, \mathrm{d}t \, \mathrm{d}t'$$
$$\leq \frac{a^2 K}{2\pi^3} \|g_s\|_\infty^2 |T|^2 \sum_{q=1}^{+\infty} \max_{u^* \in \{u_1, u_2, u_3, u_4\}} \Big(\sum_{\substack{\mathbf{n} \in \mathbb{N}^6: \\ |\mathbf{n}| = q}} a(\mathbf{n}, u^*) \Big)^2 \int_T \int_{T'} |M_r(t - t')|^q \, \mathrm{d}t \, \mathrm{d}t'.$$

Now we provide a majorant for the term $\sum_{\mathbf{n} \in \mathbb{N}^6:, |\mathbf{n}| = q} a(\mathbf{n}, u^*)$. Using (45) and the Cauchy Schwarz inequality we get

$$\sum_{\mathbf{n} \in \mathbb{N}^6 : |\mathbf{n}| = q} a(\mathbf{n}, u^*) \leq \sqrt{\sum_{\mathbf{n} \in \mathbb{N}^6 : |\mathbf{n}| = q} a(\mathbf{n}, u^*)^2 \mathbf{n}! \sum_{\mathbf{n} \in \mathbb{N}^6 : |\mathbf{n}| = q} \frac{1}{\mathbf{n}!}} \leq \sqrt{C \sum_{\mathbf{n} \in \mathbb{N}^6 : |\mathbf{n}| = q} \frac{1}{\mathbf{n}!}} \, q \|f_{u^*} \cdot \Lambda_2\|.$$

Furthermore, note that

$$\sum_{\mathbf{n} \in \mathbb{N}^6 : |\mathbf{n}| = q} \frac{1}{\mathbf{n}!} = 6! \sum_{\mathbf{n} \in \mathbb{N}^6 : n_1 \leq \ldots \leq n_6, \, |\mathbf{n}| = q} \frac{1}{\mathbf{n}!} = 6! \sum_{\mathbf{n} \in I_q(6)} \frac{1}{\mathbf{n}!}$$

where $I_q(6) := \{q \geq n_6 \geq \frac{q}{6}, n_6 \geq n_5 \geq n_4 \geq n_3 \geq n_2 \geq n_1 \geq 0, n_1 + \ldots + n_6 = q\}$. Note that $\mathrm{Card}(I_q(6)) \leq q^5$. Then, we obtain that

$$\sum_{\mathbf{n} \in \mathbb{N}^6 : |\mathbf{n}| = q} \frac{1}{\mathbf{n}!} \leq 6! \frac{q^5}{\Gamma(\frac{q}{6})}, \qquad \text{and} \qquad \sum_{\mathbf{n} \in \mathbb{N}^6 : |\mathbf{n}| = q} a(\mathbf{n}, u^*) \leq C \|f_{u^*} \cdot \Lambda_2\| \Big(q \wedge \frac{q^{5/2+1}}{\sqrt{\Gamma(\frac{q}{6})}} \Big), \tag{46}$$

for some positive constant C. It follows that, using (43), (46), and Assumption ($\mathcal{A}3$),

$$|V_{2,1}| \leq C|T|^2 \sum_{q=1}^{+\infty} q^2 \int_T \int_{T'} |M_r(t - t')|^q \, \mathrm{d}t \, \mathrm{d}t'$$
$$\leq C|T|^2 \sum_{q=1}^{+\infty} \frac{C_M^q q^2}{\mathrm{dist}(T, T')^{\gamma q - 2}} \int_T \int_{T'} \frac{C_M^2}{(1 + \|t - t'\|)^2} \, \mathrm{d}t \, \mathrm{d}t' \leq C_{2,1} \frac{|T|^2}{\mathrm{dist}(T, T')^{\gamma - 2}}.$$

It follows that $V_{2,1} = o(|T|^2)$.
Similarly for $V_{2,2}$, using (46) and Assumption ($\mathcal{A}3$) we get

$$|V_{2,2}| \leq |T|^2 \frac{Ca^2Ke^6}{4\pi^3} \|g_s\|_\infty^2 \|f_{u^*} \cdot \Lambda_2\|^2 \int_T \int_T \frac{\mathrm{d}t\,\mathrm{d}s}{(1+\|t-s\|)^2} \sum_{q=1}^{+\infty} C_M^q \frac{q^7}{\Gamma\left(\frac{q}{6}\right)},$$

which is $O(|T|^2)$ using that the series is convergent: from Stirling we get $\Gamma(q/6)/\Gamma((q+1)/6) \asymp \left(\frac{6e}{q}\right)^{\frac{1}{6}} \to 0$ as $q \to \infty$. Gathering all terms, it follows that $V_2 = O(|T|^2)$.
Terms V_3 and V_4 should be handled using the diagram formula, we conjecture that $V_3 = o(|T|^4)$ and $V_4 = o(|T|^4)$.

B Additional numerical results

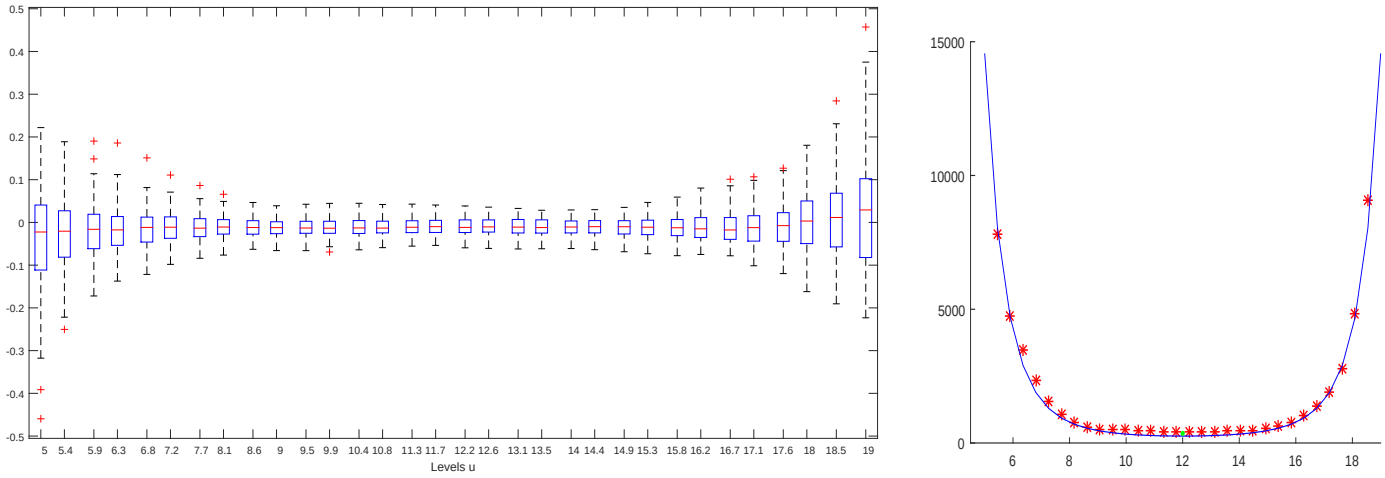

Figure 9: Synthetic digital mammograms study. Boxplot for $\widehat{s}_{u,T} - s_u$ for different values of u (left panel). Empirical variance $\sigma^2_{s_u}$ (red starts) and theoretical $u \mapsto \sigma^2_{s_u}$ in (13) in blue line (right panel). These samples have been obtained with `Matlab` using circulant embedding matrix.

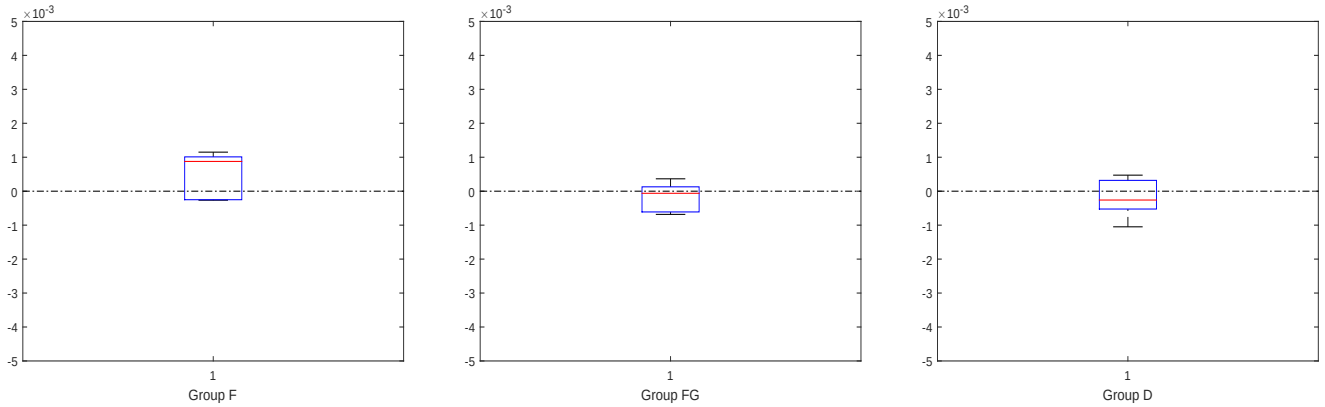

Figure 10: Synthetic digital mammograms study. Boxplots of the estimates $\widehat{C}_{0,T}(\widetilde{u})$ in (10), for each group of images (group (F) in left panel, (FG) in center and (D) in right one) with adaptive levels $\widetilde{u}$, such that for each $\widetilde{u}$ it holds that $|\widehat{s}_{\widetilde{u}}| < \epsilon$, for $\epsilon = 10^{-2}$.

Groups	$\alpha = 0.2$	Intra-class Analysis			
F	Image	2.F	3.F	4.F	5.F
	1.F	118	153	153	**204**
	2.*F*		89	126	**226**
	3.*F*			117	**211**
	4.*F*				**250**
FG	Image	2.FG	3.FG	4.FG	5.FG
	1.FG	14	105	2	4
	2.FG		74	58	21
	3.FG			129	123
	4.FG				5
D	Image	2.D	3.D	4.D	5.D
	1.D	3	8	168	110
	2.D		82	190	188
	3.D			70	5
	4.D				48

$\alpha = 0.2$	Inter-classes Analysis				
Image	1.FG	2.FG	3.FG	4.FG	5.FG
1.F	**1000**	**1000**	**1000**	**1000**	**1000**
2.F	**694**	**1000**	**1000**	**712**	**1000**
3.F	**686**	**1000**	**1000**	**715**	**1000**
4.F	**641**	**1000**	**1000**	**633**	**818**
5.F	**1000**	**1000**	**1000**	**1000**	**1000**
Image	1.FG	2.FG	3.FG	4.FG	5.FG
1.D	**1000**	**1000**	**1000**	**1000**	**1000**
2.D	**1000**	**774**	**1000**	**1000**	**890**
3.D	**1000**	**1000**	**1000**	**1000**	**1000**
4.D	**1000**	**1000**	**1000**	**1000**	**1000**
5.D	**1000**	**1000**	**1000**	**1000**	**1000**
Image	1.D	2.D	3.D	4.D	5.D
1.F	**1000**	**1000**	**1000**	**1000**	**1000**
2.F	**1000**	**1000**	**1000**	**1000**	**1000**
3.F	**1000**	**1000**	**1000**	**1000**	**1000**
4.F	**1000**	**1000**	**1000**	**1000**	**1000**
5.F	**1000**	**1000**	**1000**	**1000**	**1000**

Table 2: Synthetic digital mammograms study. Number of $p-$values associated to the 1000 different values of u that are smaller than the significant level $\alpha = 0.2$. The numbers larger than $\alpha \times 1000 = 200$ for which H_0 is rejected.